Review

Electrochemical Design of Iron-Based Advanced Materials from Complexing Electrolytes

Natalia Tsyntsaru *, Henrikas Cesiulis *, Oksana Bersirova

Posted Date: 9 December 2024

doi: 10.20944/preprints202412.0663.v1

Keywords: iron-based materials; electrodeposition; complexing electrolytes; refractory alloys; advanced properties

 doi:10.20944/preprints202412.0663.v1

Review

Electrochemical Design of Iron-Based Advanced Materials From Complexing Electrolytes

Natalia Tsyntsaru [1,2,*], Henrikas Cesiulis [1,*] and Oksana Bersirova [1]

[1] Faculty of Chemistry and Geosciences, Vilnius University
[2] Institute of Applied Physics, Moldova State University
* Correspondence: ashra_nt@yahoo.com (N.T.); henrikas.cesiulis@chgf.vu.lt (H.C.)

Abstract: Nowadays, there is a growing focus on sustainability, characterized by making changes that anticipate future needs and adapting them to present requirements. Sustainability is reflected in various areas of materials science as well. Thus, more research is focused on the fabrication of advanced materials based on earth-abundant metals. The role of iron and its compounds is particularly significant as iron is the second most abundant metal on our planet. Moreover, the electrochemical approach provides a rather eco-friendly way for versatile materials synthesis, including iron-based materials that can be found in various applications, due to a smart tuning of properties by codeposition of appropriate compounds with iron. Thus, highlighting and boosting its magnetic, catalytic, mechanical, antimicrobial/antibacterial properties, thermal, wear, and corrosion resistance. Among iron-based materials, those with refractory metals, including tungsten-based alloys, are widespread research fields with practical possibilities. Special attention in this review is devoted to peculiarities of electrodeposition from complexing electrolytes of such materials as they can meaningfully impact the final structure, content, and design of properties.

Keywords: iron-based materials; electrodeposition; complexing electrolytes; refractory alloys; advanced properties

1. Iron-Based Materials: Unlocking Sustainable Options for Versatile Applications

Nowadays, growing consideration is set on sustainability, characterized by viable changes that enable foreseeing future needs and adjusting them to the present necessities [1]. Sustainability aspects are rising in different branches of materials science too. Thus, there is an increased amount of research focused on the fabrication of advanced materials based on earth-abundant metals (iron, nickel, and cobalt), especially for catalytic applications [2,3]. Moreover, the role of iron and its compounds is significant because iron is the second most earth-abundant metal on our planet. They can be found in various applications, which will be discussed below, but certainly, magnetic [4], and catalytic [5,6] properties of iron-base advanced materials are acknowledged foremost. On the other hand, due to its proven biocompatibility and mechanical properties, iron is an excellent source material for clinical cardiac and vascular applications [7]. However, its relatively low degradation rate limits its use for the healing and remodeling of diseased blood vessels. To address these issues, a multi-purpose fabrication process was employed to develop a bilayer alloy composed of electroformed iron and iron-phosphorus [8]. In addition, alloys possessing antimicrobial/antibacterial properties such as Fe-Ag and Fe-Au have been a point of interest for the research community [9–11].

The synthesis of iron-based materials can be realized by various solid-state techniques, among which electrodeposition is often considered a smart alternative. Indeed, electrodeposition is a well-accepted surface modification method that improves the decorative and functional characteristics of a wide variety of materials. Thus, the alternation of such variables as electrolyte composition, pH, temperature, agitation, current density, potential [12–18], and even the application of a magnetic field [19] will tune the composition and microstructure, and interrelated properties of the deposited materials in a wide range.

 doi:10.20944/preprints202412.0663.v1

The electrodeposition of several types of iron alloys has been under significant attention in recent decades for magnetic application. The iron-based alloys most frequently used for magnetic applications are alloys of iron with nickel and cobalt [20]. Particularly, electroplating methods for depositing industrially valuable magnetic alloys such as Fe-Ni, Fe-Zn, Fe-Co [20,21], and Fe-Pt were researched [22]. Besides, Fe-Pd alloys possessing high perpendicular magnetic anisotropy and ferromagnetic shape memory [23,24], magnetostrictive Fe-Ga alloys [25,26], soft magnetic alloys such as Fe-W, Fe-Mo, Fe-Co-W (Mo), Ni-Fe-W see for ex.: [27–33]. Nonetheless, according to the European Chemicals Agency, nickel and Co(II) salts are substances of high concern [34]. In this view, Fe-Sn alloys were electrodeposited as an alternative to conventional magnetic nickel or cobalt-based materials [35,36]. Fe-Sn alloys can form intermetallic compounds from which ferromagnetic iron-rich of the following compositions Fe_3Sn_2, Fe_5Sn_3, and Fe_3Sn are of interest to industrial applications due to affordable cost and sustainability aspects [37]. Other magnetic iron alloys, such as Fe-P alloys [38–41] and less common Fe-Re [42] were also investigated.

The advancements in green chemistry and engineering are driving us toward the implementation of new processes or redesigning existing ones. The development of 3d transition metal-based catalysts, particularly those based on earth-abundant metals like iron, has been scientifically proven over decades and is even more important now [43,44]. Due to their adjustable chemical reactivity, catalytic efficiency, and corrosion resistance [45], iron-based catalysts have been widely studied for various applications including water purification (e.g., Fe-Mn alloys and electrodeposited zero-valent iron for Fenton reaction) [46–48], CO_2 removal (e.g., Fe-Ni nanoalloys) [49], and oxygen reduction (e.g., Fe-Co-Pt alloys) [50].

If considering corrosion properties, the fabrication of composite materials is one of the common approaches, which enables combining the useful properties of the second-phase particles with those of the metallic matrix, thus rendering a novel material with tailored characteristics. Composite coatings with alumina particles have been the most extensively studied among particle-reinforced composites. Thus, electrodeposited composite iron-based coatings such as Fe–W/Al_2O_3 [51,52] or Ni-Fe/Al_2O_3 [53] have been studied and evaluated as an effective sustainable alternative to electrodeposited hard chromium coatings. Also, Ni-Fe/WC composites have improved resistance to corrosion in comparison with their Ni-Fe counterparts [54].

One of the main peculiarities of alloys obtained by electrodeposition is the formation of solid solution phases of metals, which often cannot be predicted from a phase diagram, i.e., the formation of oversaturated solutions. Thus, during electrodeposition, the thermodynamically unstable structures of alloys are forming. By annealing them, the structural relaxation and recrystallization processes take place, so the grain size, microstructure, and properties of electrodeposited alloys can be altered considerably due to the heating of the material. In the case of iron-based advanced materials, this leads to increased recrystallization temperature, typically ranging from 400 to 600 °C [55–58]. This provides an instrument for smart tuning the properties of such alloys by varying the heating temperature and further including them as materials in thermo-resistant applications.

Though several review articles have been published on different aspects of iron-group materials, the present review aims to discuss the peculiarities and possibilities of electrochemical design of iron-containing alloys from complexing electrolytes, the advanced properties associated with those alloys, and the perspectives on the future development of the electrodeposited materials.

2. Codeposition of Metals and Peculiarities of Iron-Based Alloys Electrodeposition From Complexing Electrolytes

The thermodynamic conditions for the alloy electrodeposition are quite well understood from the macroscopic standpoint. This approach is comprehensively discussed in [17,59–62]. The key point in the macroscopic thermodynamic description of alloy electrodeposition is an analysis of the Nernst equation written for the equilibria between metal ions in the solution and metal (origin or foreign). Due to the activities of elements in the alloy differing from the unit, the Nernst equations for the two

 doi:10.20944/preprints202412.0663.v1

equilibria alloy/solution of the electroreduction of a binary[1] alloy for metals A and B can be presented as:

$$\mathrm{A}^{z_A+} + z_A e^- \rightarrow \mathrm{A}_{\mathrm{alloy}}$$
$$B^{z_B+} + z_B e^- \rightarrow \mathrm{B}_{\mathrm{alloy}} \quad (1)$$

where the equilibrium potentials, $E^{(i)}_{eq,alloy}$ for each alloying component can be written as follows:

$$E^{(A)}_{eq,alloy} = E^{0'}_A + \frac{RT}{z_A F}\ln\frac{a_{A^{z_A+}}}{a_{A,alloy}}$$
$$E^{(B)}_{eq,alloy} = E^{0'}_B + \frac{RT}{z_B F}\ln\frac{a_{B^{z_B+}}}{a_{B,alloy}} \quad (2)$$

where: $E^{0'}_A$ and $E^{0'}_B$ is a formal potential of components mentioned above A and B, respectively;

$a_{A^{z_A+}}$, $a_{B^{z_B+}}$, $a_{A,alloy}$, $a_{B,alloy}$ is the activity of ions in the solution and components A and B in the alloy, respectively; other marks are standard.

The most favorable conditions for the alloy electroforming of two metals A and B are usually achieved when the equilibrium potentials' values are close. In this case, the equilibrium composition of the alloys can be expressed by equilibration of eq. 1 and 2, and might be represented as follows:

$$\frac{a^{z_A}{}_{A,alloy}}{a^{z_B}{}_{B,alloy}} = \frac{a^{z_A}{}_{A^{z_A+}}}{a^{z_B}{}_{B^{z_B+}}}\exp\left[\frac{F}{RT}\left(E^{0'}_B - E^{0'}_A\right)\right] \quad (3)$$

As seen from eq. 3**, the composition of alloys depends on the activities (or concentrations) of metal ions in the solution. Notably, the activity coefficients can be neglected for moderately dilute solutions (up to 1–2 M), and concentrations of components are used instead of ones since they appear in the Nernst equation in the logarithmic form. Thus, for example, if the activity coefficient is only 0.8, instead of an assumed value of 1.0, the resulting error in the value of E_{eq} is only (5.7/z) mV (where "z" is the number of electrons transferred in the reaction per molecule). Therefore, in many cases, the concentrations are used instead of activities in the thermodynamic equations [59].

The presence of various complexing agents in solutions decreases the concentrations of solvated "simple" metal ions, leading to a negative shift in the equilibrium potentials. Here, we should dive into how this negative shift is formed in the complexing electrolytes of a metal (M).

The equilibrium in the solution phase contained complexes is settled between free metal ions M^{z+}, free ligand L, and various complexes ML_j^{z+}:

$$\mathrm{M}^{z+} + \mathrm{jL}^{m} \Leftrightarrow \mathrm{ML}_{\mathrm{j}}^{z+\mathrm{jm}} \quad (4)$$

where: j= 1…. n; m is a charge of ligand.

In the simplest case, when a single complex can be formed in the solution, such equilibria may be represented by the equilibrium constant called cumulative stability constant (β_n), which can be presented as:

$$\beta_n = \frac{\left[\mathrm{ML}_{\mathrm{n}}^{z+\mathrm{nm}}\right]}{\left[\mathrm{M}^{z+}\right]\left[\mathrm{L}^{m}\right]^{j}} \quad (5)$$

If stable complexes are formed, the value $\beta_n >> 1$. Usually, the concentration of ligands in the solution is higher than the total metal concentration. Therefore, it essentially reduces the concentration of free metal ions in the solution

---

[1] For simplicity, the binary alloys are described. However, the same approach can be applied to the multicomponent alloys (ternary, quarterly, etc.).

** Please note, that the equation is expressed differently in [60].

 doi:10.20944/preprints202412.0663.v1

$$\left[\mathrm{M}^{z+}\right] = \frac{1}{\beta_n} \cdot \frac{\left[\mathrm{ML_n^{z+nm}}\right]}{\left[\mathrm{L^m}\right]^j} \quad (6)$$

and causes an essential negative shift in equilibrium (thermodynamic) potential

$$E_{eq}^{(M)} = E_M^{0'} + \frac{RT}{zF} \ln\left(\frac{\left[\mathrm{ML_n^{z+nm}}\right]}{\left[\mathrm{L^m}\right]^j}\right) - \frac{RT}{zF} \ln \beta_n \quad (7)$$

Consequently, it also causes the negative shift of the metal deposition potential, E_{dep}, to more negative values:

$$E_{dep}^{(M)} = E_M^{0'} + \frac{RT}{zF} \ln\left(\frac{\left[\mathrm{ML_n^{z+nm}}\right]}{\left[\mathrm{L^m}\right]^j}\right) - \frac{RT}{zF} \ln \beta_n + \eta \quad (8)$$

The term η in eq. 8 represents the difference between deposition and equilibrium potentials:

$$\eta = E_{dep}^{(M)} - E_{eq}^{(M)} \quad (9)$$

and is crucial for understanding the possibilities of alloy electroforming. However, precisely predicting the composition of electrodeposited alloys based only on thermodynamic data is quite complex due to the kinetic peculiarities of metals' electrodeposition. The complexing electrolytes for metals and alloys electrodeposition are essential because the formation of complexes decreases the exchange current density (η increases) and could lead to the improved uniformity, smoothness, and brightness of the deposits [59].

On the other hand, to investigate successfully the electrochemical processes at the metal/solution interphase in the presence of complexing agents, attention should also be paid to the solution chemistry. In other words, it is necessary to evaluate the distribution of complexes and ligands in the solution volume. For this purpose, it is possible to extract concentrations of all species formed in the solution after the dissolution of corresponding salts by solving the system of equations using commercially available software e.g., Maple6, MathCad, MINDTEQ, Meduse, or others. The set of the system of equations has to include the following relations and quantities:

(i) the equilibrium constants for all compounds added to or formed in the solutions: acids deprotonation, hydrolysis, polymerization, stability constants of metal complexes with ligands, etc.;
(ii) the mass balance equations $[J]_{tot} = \sum \left[J_i^{n+/-}\right]$ for all forms in the equilibrium mixture, and
(iii) the charge balance "Cat" and "An" denote cation and anion, respectively.

Certainly, the calculated distributions of species in the electrolyte can vary depending on the concentration of precursors and pH, leading to changes in the deposit composition and properties respectively. Thus, evaluating the distribution of species in the citrate and tungstate-based electrolytes, cca 20-32 various species depending on pH were found and used for calculation, which led to:

(i) the formulation of a thermodynamically stable solution for Fe-W electrodeposition from the Fe(III)-based compounds and the electrodeposition of Fe-rich or W-rich advanced materials (**Figure 1**) with rather high current efficiency (CE) [63,64];
(ii) the understanding of the correlation between W content in the Co-W alloys as a function of pH and forming citrate complexes of WO_4^{2-} [27];
(iii) the determination of conditions that allow an increase in the deposition rate of Ni-W alloys [65];
(iv) the impeding of the deposition of Ni during Ni-W alloy electrodeposition [59];

Preprints.org (www.preprints.org) | NOT PEER-REVIEWED | Posted: 9 December 2024 doi:10.20944/preprints202412.0663.v1

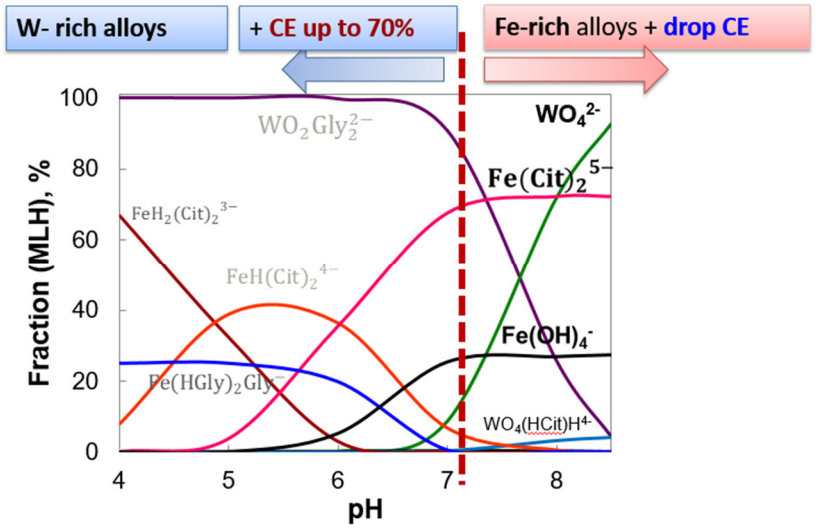

Figure 1. Calculated distribution of various complexes in the glycolate-citrate electrolyte vs. pH (based on the data reported in [63], and variation of tungsten/iron content and current efficiency of Fe-W electrodeposits.

Furthermore, the evaluation of species distribution in the complexing electrolytes allowed authors to clarify the following:

(v) the pH range for stable ferric-stannous tartrate-chloride-sulfate electrolytes for Fe-Sn electrodeposition [35];
(vi) the role of glycine in the Fe-P alloy electrodeposition [66];
(vii) the codeposition conditions, e.g., for CoFeNiCu alloys electrodeposition from citrate solutions [67];
(viii) to design Pourbaix diagrams for systems containing few metals and complexing agents, e.g., for Cu-Co-Fe in acetate solutions [68], for Fe–V–O–H system [69].

Here, should be considered that complexes play an important role in controlling structure, composition, and the materials' properties due to their direct involvement in the formation of electroactive species in the bulk or on the electrode surface during deposition. Thus, the well-known peculiarity associated with the electrodeposition of materials containing iron group metals with refractory metals mentioned above is linked to the mechanism of codeposition of such materials, which is classified as induced codeposition [70,71], contrary to anomalous [72] that is regular to the iron-group metals codeposition (e.g., FeNi alloys) or their codeposition with Zn or Cd. The understanding of the induced codeposition mechanism and the role of complexes in the case of refractory metals codeposition was overviewed elsewhere [27,59]. We will not enter into a deep discussion on this matter here, it can only be specified that either "bulk" and/or "adsorbed" complexes formed during induced codeposition could be correlated to the experimentally observed results.

However, while developing iron-based materials with rhenium under an induced codeposition mechanism some particularities should be considered, namely, in contrast to WO_4^{2-}, perrhenate ions (the source of rhenium) do not form polynuclear complexes in acidic solutions. Therefore, depositing rhenium with iron group metals is possible, preferably using citrate-based weakly acidic or neutral solutions. The compositions of electrolytes, electrodeposition conditions, compositions of obtained alloys, and their properties can be reviewed in [59,73,74].

Also, it should be considered that the standard reduction potential (E_o^{red}) of Re in the perrhenate ions solutions is +0.363 V at pH 0, and the Nernst potentials are -0,110 V at pH 7, and –0.584 V at pH 14.0. These values are more positive than that for the iron group metals, e.g., E_o^{red} for Fe^{2+}/Fe and Fe^{3+}/Fe are -0,447 V and -0,037 V, respectively [75]. However, the electroreduction of ReO_4^- is highly irreversible. The ReO_4^- reduction wave occurs just before the onset of electrolyte decomposition, but

 doi:10.20944/preprints202412.0663.v1

electroreduction in weakly acidic citrate or oxalate solutions is facile, resulting in a polarographic wave at much more positive potentials. Authors explain this fact by forming electrochemically active $(ReO_4 \cdot H_2Cit)^{2-}$ complexes at pH above 3 [76]. The role of this complex in the codeposition mechanism of Re with Fe has been discussed in [59,74]. However, based on the UV–vis absorption spectroscopy data obtained in the citrate-perrhenate system at pH 5 indicated that the ReO^{4-} ions are unlikely to chemically bind to the dissociated citric acid. Therefore, it is assumed here that even in the presence of citrate ions, the ReO_4^- ion remains hydrated [77]. In that respect, it is an interesting consideration that the overall reaction leading to the formation of rhenium is influenced by the presence of H^+ ions which depend on the adsorption process and therefore of the electrode surface nature. This means that the surfaces with high adsorption of hydrogen could facilitate the reduction of perrhenate ions to Re [78].

Moreover, to explain some results of experimental studies on induced codeposition, a new theoretical approach was developed, in which the existence of an N-dimensional fractal cluster in the solution is assumed [79]. The given theory enables us to avoid the difficulties of the classical theory of nucleation operating with the concepts of surface energy, which is intrinsic to a geometrical surface. In this case, the electrochemical kinetics of nucleation, rather than electrochemical reaction is considered. In this sense, the nucleation stage should be considered as the step following the formation of an ad-particle on the surface.

By applying a non-linear approximation of nanonucleation from fractal solutions for interpretation of induced codeposition of iron group alloys with refractory metals, it was possible to explain that a high rate of propagation of crystallisation front influence on:

(i) nanocrystallinity of the electrodeposited new phases;
(ii) formation of composites containing oxide-hydroxide inclusions;
(iii) absorbed hydrogen at high current density.

Another peculiarity that should be taken into account is the stability of Fe (II) species in the developed electrolytes [80]. The stability of electrolytes containing iron salts can often hinder the usage of iron-based materials for scale-up applications. Electrolytes based on Fe(II) salts are unstable thermodynamically and the solution content is governed by the Fe(II) oxidation kinetics [20].

It was shown that citrates and ammonia [20] inhibit the kinetics of Fe(II) oxidation to Fe(III), but cannot prevent it. Some attempts were made to prolong bath life by adding reducing agents, such as L-ascorbic acid [80,81] but those compounds can affect the bath maintenance and coatings properties. In the case of Fe-Ag alloy electrodeposition an instability caused by the reduction of Ag(I) by Fe(II) was partially resolved by adding 1% Fe^{3+} [11]. Unless used regularly, the solution containing Fe(II) will oxidize gradually, and the time and effort required to restore the electrolyte to an operable condition may outweigh the economic benefit of depositing a lower-cost material; e.g., it is necessary to reduce the Fe(III) ion before using a freshly prepared bath, and this process might require 24–48 h [20]. Therefore, the electrodeposition of Fe-alloys, from the solutions based on Fe(III) compounds, was also investigated for the fabrication of Fe-W, Fe-Ni, Fe-Pt, and ternary alloys [63,82–85].

3. Versatile Materials Based on Iron-Based Alloys

In this section, the main focus will be given to practical aspects of electrodeposited iron-based alloys with refractory metals (mainly tungsten-based) as these alloys can be adapted for versatile applications.

From an application point of view, iron-based alloys with refractory metals are an important class of functional materials that are characterized by a distinctive set of properties linked to the presence of high melting refractory metal, such as increased heat resistance and stability at high temperatures, high corrosion resistance, and excellent mechanical properties [27,86–88]. Refractory-metal-containing alloys are advanced materials for strategic components in many industries (hard coatings, catalysts, aerospace, chemical, nuclear, defense, biomedical, etc.), including as a component of superalloys [89]. The codeposition of refractory metals with iron group metals leads to obtaining high-quality electrodeposits with higher current efficiencies [56,63,90], and in many cases, can replace

 doi:10.20944/preprints202412.0663.v1

high-cost materials. However, the research on iron alloys is still growing compared to other metals due to the sustainability aspects and advanced properties of iron-based materials.

3.1. Structural Peculiarities, Mechanical, Thermal Resistance, and Magnetic Properties

3.1.1. Structural Peculiarities and Mechanical Properties

The key factors affecting the properties of the electrodeposited material are linked directly to its structure and chemical composition, and the electrochemical approach induces the precise scenario for an alloy synthesis with targeted amorphous and/or nano-structure, composition, internal ordering, and texture. Thus, the main characteristic of electrodeposited iron-based materials with refractory metals is their nanocrystalline structure, which primarily impacts those alloys' hardness [29,31,51,56]. This impact is correlated to refractory metal content in the electrodeposit and the reduction of crystallite size. Thus, according to the Hall–Petch relation, usually, the mechanical properties will advance with decreasing the grain size due to grain boundaries increase, which minimizes dislocation motion. Moreover, effects such as nanostructuring and solid solution strengthening will also be involved.

However, there is a critical value of crystallite size at which the Hall–Petch relation will be distorted. In the case of Co-W [91] and Ni-W [92] alloys, the breakdown occurs at crystallite sizes of 5 nm and 10 nm respectively. Notably, the same tendency was also observed in the case of more complex systems such as e.g., high entropy NiFeCo-W alloys [93]. Remarkably, this often corresponds to the transition to the amorphous-like or ultra-nanocrystalline structure of electrodeposited materials [94], which promotes the diverging of the shear bands that lead to the nanohardness decrease. However, the ultra-nanocrystalline structure brings other benefits, e.g., it can increase catalytic properties, which will be discussed later below.

Moreover, the hardness of Fe-W increases from 4.1 GPa (alloy having 6 at.% W) to 10.4 GPa (alloy having 25 at.% W), and consequent increase in the elastic modulus from 83 to 216 GPa. This trend is strongly correlated to the formation of a stable intermetallic phase of Fe_2W which results in the advanced hardness for the coatings containing more than 16 at.% of W [29]. As a result, smart tuning of mechanical properties can be accomplished by varying alloy composition and applied experimental conditions (**Figure 2**). Concerning alloy composition, it can be underlined that under the same testing conditions and equal refractory metal content, generally, iron-based alloys have higher hardness than cobalt or nickel-based electrodeposited materials [56], which encourages the use of iron-based materials for hard coating applications.

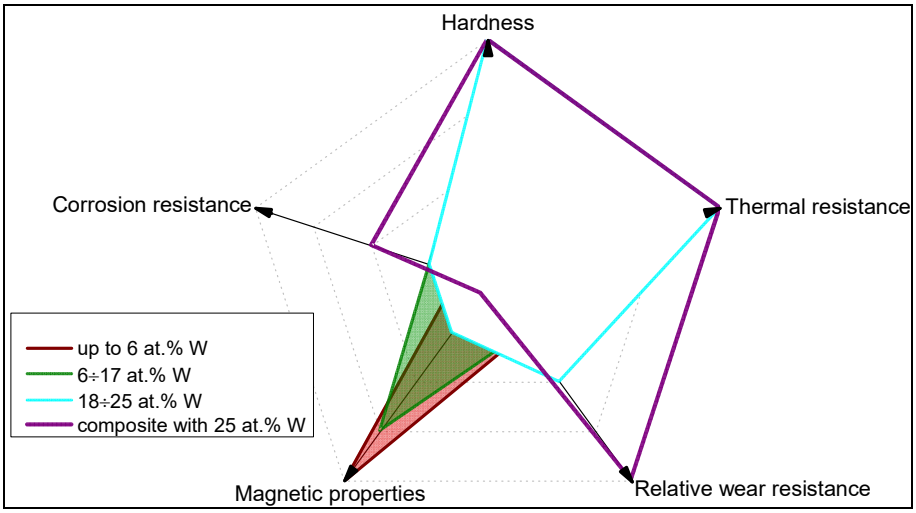

Figure 2. Properties mapping of electrodeposited Fe-W alloys as a function of tungsten content in the coating. In addition, properties of Fe-W/Al_2O_3 composited coating are presented for comparison. The black arrows show the increase in the corresponding characteristics (a.u.). The Fe-W alloys were electrodeposited from environmentally sustainable glycolate-citrate electrolyte [63].

 doi:10.20944/preprints202412.0663.v1

On the other hand, experimental conditions namely, volume current density (VCD) can also affect drastically the hardness and even corrosion as demonstrated in [95–98]. The VCD describes the ratio of current to the volume of an electrolyte (I/V). It is an important characteristic especially taking into account the upscaling of lab processes, because usually only common characteristics such as pH, composition, temperature, current density, or potential are considered. The dependence of alloy composition on VCD is linked to a different rate of the metal complex (gluconate, citrate, etc.) concentration change during induced codeposition. VCD is mainly specific to induced codeposition of tungsten alloys, while it does not influence the electrodeposition of industrially important metals such as nickel or chromium from non-complexing electrolytes [95].

During the codeposition of refractory metals, significant differences in composition, morphology, and microhardness may occur depending on the electrolyte volume, at either constant electrode potential or current density [96]. Thus, depending on VCD, electrodeposited nanocrystalline alloys contain not only iron group and refractory metals, but also different amounts of intercalated oxides and hydroxides, and even alloyed hydrogen (e.g., Fe-W-H) [96,99], that ultimately will impact on the properties. Another important experimental parameter is the nature of the counter electrode (material from which the anode is made and if it is insoluble or soluble). It affects intrinsic and extrinsic characteristics of refractory metal alloys during induced codeposition from complexing electrolytes, including the rate of deposition, and hardness [97,100].

3.1.2. Thermal Resistance

The presence of inclusions and abundant evolution of hydrogen during electrodeposition can promote brittleness in obtained iron-based materials [87]. In this view, annealing can decrease the internal stress of the deposits and advance the mechanical properties. During annealing, electrodeposited refractory alloys will recrystallize forming coarser grains and new phases (oxides, intermetallic phases, carbides, etc.) [55–57,64,101,102]. Characteristically refractory-rich alloys (with a high content of refractory metal) have improved thermal resistance linked to the formation of thermodynamically stable nanostructures with decreased energies of segregation and grain boundary. For instance, the XRD amorphous-like structure of Fe-W alloys can withstand temperatures up to 600 °C, which is higher than for Ni-W or Co-W alloys with the same tungsten content [56,64]. Above this temperature, a partial recrystallization occurs in the Fe-W alloys, but some amorphous peaks still are presented in XRD patterns even at 800°C [103]. The nanocrystalline peaks of annealed alloys usually are attributed to α-Fe, Fe_2W, $FeWO_4$, and Fe_6W_6C phases [103,104], although Fe_7W_6 phase [105] can be also present in the as-deposited coating having a more coarse-grained structure and lower tungsten content. However, in tungsten-rich alloys, electrodeposited from citrate-based electrolytes, uncommonly seen phases such as Fe_6W_6C and Fe_3W_3C have been also detected after heat treatment at 700°C [104] and 800°C [103].

The appearance of hydrogen, carbon, and oxygen-containing phases (**Figure 3**) is mostly attributed to the deposition from complexing electrolytes having organic ligands, which afterward affect the microstructure and properties of as-deposited and annealed alloys [103,104,106,107].

 doi:10.20944/preprints202412.0663.v1

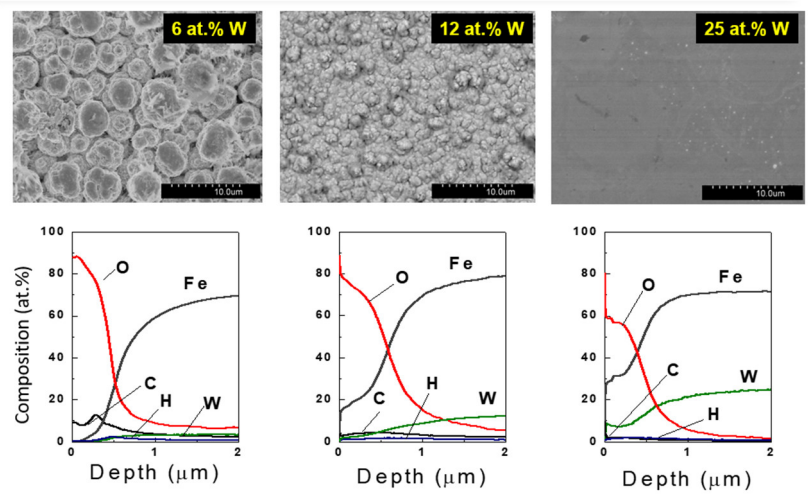

Figure 3. The representative SEM images of Fe-W alloys having different amounts of tungsten (indicated on the images) and the distribution of light elements (obtained by GD-OES) in the top layer of the 10 μm coating for corresponding electrodeposited materials.

Moreover, the dependence of annealed alloy properties (hardness, wear, and corrosion resistance) on temperature usually will have an optimum. This optimum for heat treatment will depend on the initial tungsten content in the coating and the "amorphous state" of as-deposited Fe-W coatings, which is connected to a shift of the annealing temperature from 500°C [105] to 600°C [103] and 700 °C [104]. Also, it is connected to the precipitation and dispersion of fine α-Fe crystallite and Fe_3W_3C particles in the Fe-W alloys [108]. Thus, this leads to a hardness increase from ~8÷10 GPa for the as-deposited coatings having 25÷36 at.% of W to ~16 ÷ 20 GPa for annealed ones. At higher temperatures such as 800 °C coarse grains are formed which negatively impacts the hardness of the material [103,107]. Overall, we should emphasize that the increased content of refractory metal in iron alloys will facilitate a transition to a more thermal-resistant state of deposited materials (**Figure 2**).

3.1.3. Magnetic Properties

Electrodeposited Fe-based alloys are extensively studied for applications in magnetic devices because it is possible to tune both the composition and structure of obtained materials. To achieve the optimal soft magnetic properties, grain size control is critical. According to a model proposed by Herzer [109], coercivity H_c is proportional to the sixth power of average grain size, i.e., so-called "*D6*" law. As was shown in [110], for Co-Fe alloys electrodeposited from citrate-based baths, the average grain sizes in deposits are around 10–20 nm, which is quite fine and beneficial for achieving optimal soft magnetic properties; so, the CoFe films electrodeposited from citrate-added baths exhibited better soft magnetic properties than those deposited from citrate-free baths under the applied experimental conditions. A similar behavior was obtained for $Ni_{86,0}Fe_{9,8}W_{1,3}Cu_{2,9}$ alloy electrodeposited from citrate baths: during annealing the mean crystallite size increased from 12 to 29 nm resulting in reduced magnetization and broadened magnetic hysteresis and thus increased loss of the active power and decreased the strength of the coercive field [111]. Electrodeposited from citrate bath CoFeNi thick films also obey a "*D6*" law for the correlation between crystallite size and coercivity, but the saturation magnetization is not influenced by the crystallite size and depends on the chemical composition [112]. However, in the case of electrodeposited Fe-Pd alloys from citrate-ammonia baths, as deposited alloys are almost disordered, whereas annealing at 400-600 °C promotes crystallinity, and the magnetic coercitivity increases up to 10 times [113].

Exploration of soft magnetic iron-based alloys such as NiFeCo can be further extended by the incorporation of rare earth elements (e.g., Tb and Dy), which contribute to giant magnetostriction of electrodeposited materials that can be engaged in resonant frequency sensing devices [114]. In

 doi:10.20944/preprints202412.0663.v1

addition, a magnetic field applied during the electrodeposition can provide a feasible way to produce oriented magnetostrictive CoFe materials for dual-mode flexible sensors [115].

In the case of iron-based materials with tungsten, the magnetic properties are very largely dependent on electrochemical design. Thus, the experimental conditions (pH, deposition temperature, current/potential) will affect the structure, composition, and, in the end, the transition to a semi-hard or soft magnetic nature of deposited materials. Thus, hard and soft magnetic properties of refractory binary [91,116,117] and ternary [33,118–120] alloys, and more complex systems [121] with iron have been reported. The hard and soft magnetic properties are more likely to be found in cobalt-based alloys [91], while iron-based alloys with refractory metals are generally characterized by a low coercive field (Hc<200 Oe). Therefore, soft or semi-soft magnetic properties could be expected, which can be applied to sensors, read/write heads in hard discs, and microelectromechanical systems.

Here, we should underline that, commonly, with an increase in the non-magnetic phase (refractory metals in our case), the saturation magnetization will decrease. Thus, Fe-W alloys electrodeposited at room temperature display a much sharper decrease in saturation magnetization for deposits having 12 at.% of W, but deposition at 65 °C (16 at.% of W) leads to retention of rather high magnetization [29]. This behavior is attributed to the thermodynamic constraints of nucleation and crystallite phase formation from complexing electrolytes at room and elevated bath temperatures. Thus, an amorphous-like structure can be formed at room temperature at a lower content of refractory metals (12-14 at.% of W). However, at higher temperatures, the XRD amorphous peaks start to appear only at 16-18 at.% of W.

Furthermore, the nanocrystalline deposits have a higher value of the saturation magnetization caused by the presence of the α-Fe phase in the Fe-W alloy, while XRD amorphous phases such as solid solution of tungsten in iron, W(Fe), and intermetallic Fe_2W contribute to a decrease in saturation [29]. The coercivity evaluation of such materials illustrates an overall semi-soft magnetic character with values in the range 10 ÷ 190 Oe depending on tungsten content (**Figure 2**).

3.2. Wear and Corrosion Resistance

One of the important aspects of research on the iron group metals refractory alloys is connected to finding materials that can replace deposited chromium, whose synthesis involves restricted compounds of Cr (VI) [122]. Hence, iron-base alloys are an important pillar that addresses sustainable issues linked to Cr(VI) and the subsequent use of chromium as a hard and corrosion-resistant coating. Additionally, our group's research indicates that the wear rate of tungsten-based alloys under identical testing conditions is comparable to that of electrodeposited chromium. [27]. Similar data obtained under different test setups were demonstrated by other researchers [123]. In general, the comparison of the tribological behavior of different materials is quite complicated due to the involvement of different tribo-systems and test conditions. Therefore, commonly the evaluation of tribological properties is mostly linked to material characteristics, namely the ratio between hardness (or plasticity) and wear [92,124]. The higher ratio between hardness and elastic modulus (elastic strain to failure) provides a material with enhanced resistance to permanent plastic deformation, which could diminish wear caused by this deformation [124]. Indeed, elastic-plastic behavior was the prevailing cause of wear under dry friction conditions of electrodeposited Ni-W alloys [92,125]. Moreover, the formation of a stable hexagonal close-packed (hcp) structure which impedes the plastic flow in Co-W electrodeposits led to an improved wear resistance at high applied loads [27,126].

However, the tribological behavior of Fe-W alloys at dry friction conditions is primarily determined by the chemical stability of iron under fretting (its tribooxidation) and not only by mechanical characteristics [127]. Iron oxide particles that form in the wear track act as an abrasive third body, which increases the asperity contact between the material and counter-body, thus resulting in a high coefficient of friction and larger wear volume than in the case of Ni or Co-based alloys. Here, it should be taken into account that increased refractory metal content (low iron content) in the deposits and heat treatment of as-deposited alloys will increase the relative wear and corrosion resistances of iron-based materials [59,92,127].

 doi:10.20944/preprints202412.0663.v1

Another possibility to improve the wear and corrosion resistances of iron-based materials like Fe-W is to introduce a new alloying element e.g., Zn, P, La into binary alloys [128–130]. Although the tribological and corrosion properties usually improve with the increasing content of newly alloyed components, this approach will provide only a temporary remedy until iron particles start to oxidize.

However, under lubricating conditions using environmentally sustainable rapeseed oil, it was possible to substantially decrease the tribooxidation and wear of Fe-W alloys, by applying a rather thin layer of the oil (1 μm thickness) [131]. Thus, the particles of iron oxide were absent in the wear track and at the surface of the counter-body, and the roughness inside the wear track was very close to the initial surface roughness. Hence, the lubricating conditions can considerably improve the tribological characteristics of Fe-W coatings. Nevertheless, the liquid lubricant in this case must be injected regularly to extend the lifetime of the coating, which can apply only to some specific devices.

In this view, composites provide a bigger stage for innovative solutions, where already not only conductive compounds but also non-conductive ones can be codeposited [53]. Moreover, composites combine the properties of an alloy with the chemical and physical properties of second-phase particles, thus producing a material with advanced characteristics compared to its analog having the same composition (**Figure 2**) [51,52]. Usually, we can increase the hardness of the composites, which is positively affected by grain refining, dispersion strengthening, and texturing effect induced by particles. In addition, wear resistance can be also improved by choosing the appropriate composition of composites based on a metal matrix and particles such as ZrO_2, SiC, or Al_2O_3, due to the self-lubricating effect [132].

Here, it should be underlined that the introduction of the particles is not a guarantee of a composite with improved characteristics. Frequently, it can lead to increased porosity, low adhesion to the metallic matrix, and peculiarities of codeposition, which could increase, for instance, the corrosion rate. Thus, the Al_2O_3 particles in Ni-Fe/Al_2O_3 composite had overall an unfavorable influence on the corrosion resistance, due to the increased porosity, roughness, and inhomogeneity of the deposits [53]. Therefore, the smart design of composites is needed. Thus, another approach involving a trilaminar structured composite has been applied to protect the Fe-W alloy. Namely, a silane cross-linked graphene oxide layer and hydrophobic organosilane layer were formed on top of the Fe-W amorphous alloy layer to protect it against corrosion [133]. This approach provided the possibility to decrease corrosion rate up three orders of magnitude and to increase overall hydrophobic performance (contact angle was 141.7 degrees) by adjusting the morphology of the electrodeposited Fe-W alloy layer.

3.3. Catalysts Based on Electrodeposited Iron-Based Materials and Upgraded Systems

Electrodeposited alloys are widely researched as electrocatalysts for water electrolysis and other reactions. A key factor in electrocatalysis is the selection of electrode materials that demonstrate high electrocatalytic activity. This quality is essential for enhancing efficiency and reducing the costs of the process. The efficiency depends on two main factors: the composition and structure of electrodeposited material, and the electrochemically active area of the catalyst. It was confirmed that a nanocrystalline or amorphous-like/ultrananocrystalline structure of the electrode material leads to an enhancement of the electrocatalytic performance because the fine crystallites of the material increase its surface-over-volume ratio. Given that electrochemical reactions occur at the interface between a solid catalyst and an electrolyte, nanocrystalline electrodes offer a larger surface area accessible for reactants to adsorb [94].

We should highlight an important factor that influences the catalytic activity of electrodeposited coatings, namely the electrochemically active surface area (EASA). By knowing the EASA, it is possible to evaluate the intrinsic catalytic activity of the material and distinguish which of the parameters contributed to the catalytic performance of investigated electrodes, especially in the case of 3-D electrodes (electrodeposition on porous electrode, metallic foam). Electrochemical impedance spectroscopy (EIS) is an effective method to evaluate EASA.

Various parameters of EIS data can be used for the EASA estimation depending on the reactions of the catalytic process: (a) capacitance of double electric layer (reaction involves adsorbed

 doi:10.20944/preprints202412.0663.v1

intermediates); (b) Warburg impedance (reaction with limiting mass transfer rate); (c) charge transfer resistance (reactions with slow charge transfer rate, e.g., HER, OER) [134–136]. For instance, using a 3D electrode (Ni-foam) and co-doping FeW-based catalysts with Ni_3S_2/NiS it was possible to improve the catalytic performance of elaborated materials toward OER and urea oxidation [137], and towards both HER and OER [138].

As discussed earlier, electrodeposited nanocrystalline iron-based coatings with tungsten and other refractory metals are versatile materials that have also been found to be applicable in catalysis. The analysis of the electronic configuration of d-metals shows that the codeposition of two or more such metals from two branches of Balandin's volcano curve, could improve and even exceed their individual electrocatalytic properties [139]. Thus, iron-based materials have been employed as catalysts for: methanol and ethanol oxidation [140,141]; hydrogen (HER) and oxygen (OER) evolution reactions [94,142,143]; photoelectrochemical water splitting by dealloying of electrodeposited Fe-W alloy [144].

The catalytic activity of iron-based materials with tungsten is closely linked to the composition, structure/ phases of the alloys, and the pH of the working medium. Moreover, a significant improvement of the catalytic activity leading to the visible reduction of the hydrogen overpotential and the increase of the apparent exchange current density was noticed with increasing the temperature of the working medium [94]. Generally, the high content of the refractory metal and ultra-nanocrystalline structure (crystallite size below 10 nm) determines enhanced catalytic properties of such alloys coupled with reasonable corrosion resistance in acidic solutions, needed for example for methanol oxidation [94,140,145].

The high catalytic activity of the ultra-nanocrystalline tungsten alloys (containing 30 at.% of W) for HER application can also be ascribed to the formation of stable intermetallic phases [146], ensuring optimal metal distribution over the surface and producing larger catalytically active sites. However, the catalytic activity of CoW-based alloys is usually higher than that of iron-containing analogs [94], **Figure 4**.

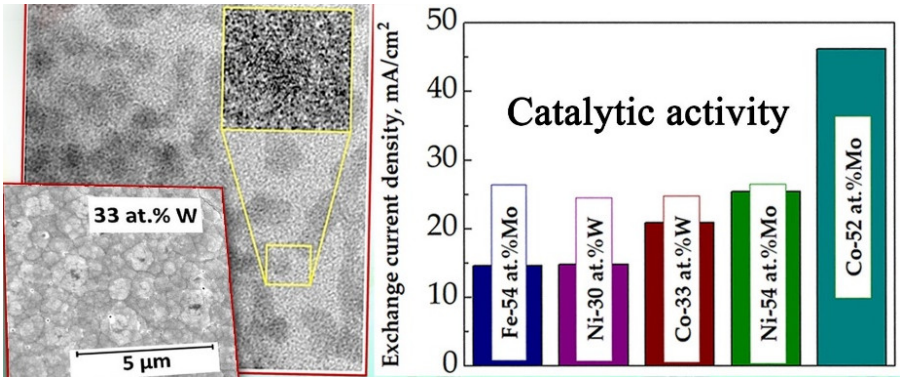

Figure 4. Representative SEM and TEM images and exchange current densities of ultrananocrystalline tungsten and molybdenum-rich iron group metal alloys.

A considerable part of research involving iron-based materials is focused on the design of effective catalysts based on Fe binary and ternary alloys with Mo [147,148] because they have the potential to be applied as an efficient HER electrocatalyst in *alkaline media*. Among effective Mo-rich (52-54 at.%) alloys, the apparent exchange current density of hydrogen evolution for Co-Mo electrodeposits was considerably higher than those for Ni–Mo and Fe-Mo coatings [149]. Furthermore, the molybdenum-rich coatings show high catalytic activity also for oxygen evolution reaction [150]. Concerning the use of rhenium iron-based metal alloys e.g., Fe-Re alloys, there are limited data on the catalytic activity of such alloys for HER and OER or other electrochemical reactions, but these alloys show superior catalytic performance compared to monometallic Fe and Re catalysts for hydrogenation reaction [151].

The new possibility to further explore the above-mentioned materials is the employment of more complex iron-based catalytic systems such as high entropy alloys (HEAs). For example, these alloys

 doi:10.20944/preprints202412.0663.v1

typically exhibit higher catalytic activity for the hydrogen evolution reaction compared to electrodeposited binary alloys. This is due to a larger number of active sites having different electronic structures and adsorption energies [152]. Commonly, the catalytic behaviour of HEAs is associated with four core effects: high entropy effect in thermodynamics [153], lattice distortion effect in structure [154], hysteresis diffusion effect in dynamics, and cocktail effect in properties [155].

Thus, the electrodeposited Ni-Fe-Cu-Co-W high entropy alloys on iron sheets due to the interaction of different elements and high mixing entropy led to the formation of a cauliflower structure on the surface that shows high catalytic activity. The excellent oxygen evolution reaction (OER) activity was derived from (1) the synergistic action between many metals that enhances the intrinsic activity; (2) the binder-free self-supporting structures provided a short diffusion channel for electrolyte penetration and faster electron transfer; (3) the special cauliflower structure on the surface of the electrode provided an increase in the contact area [156]. Moreover, the synergetic effects in the electrodeposited FeCoNiMoW high entropy alloy also deeply impact the magnetic and corrosion properties of such materials [157].

Another possibility and advantage of exploring ferromagnetic alloys as catalysts is linked to the magnetic field application during the catalytic reaction. Thus, it was possible to reduce by 10% the electricity needed for hydrogen generation, compared to the base case scenario, due to the synergetic effect of catalytic and magnetic action [158]. Moreover, the perspectives of iron-based magnetic materials as catalysts are not limited only to HER or OER reactions. For instance, the Fe-Ce-W magnetic catalyst can be smartly tuned to increase selectivity towards nitrogen oxides reduction [159]. Additionally, assessing the stability of Fe-based catalysts is vital for their long-term application in practical engineering, particularly in oxidation processes [160], aggressive media [161–163], and fuel cells [164].

4. Conclusions and Future Perspectives

We explored the potential of utilizing earth-abundant materials, specifically focusing on iron-based deposits and refractory metal alloys. The properties of these materials can be easily adjusted through careful electrochemical design. For example, by simply shifting the pH of the solution, we can affect the distribution of complex species and obtain alloys that are rich in iron or tungsten with varying current efficiency (CE), as shown in Figure 5. This process leads to different compositions, morphologies, and structures, which can also be further fine-tuned by precisely controlling the temperature of the electrolytic baths. This control allows for transitions between nanocrystalline, ultrananocrystalline, or amorphous-like structures.

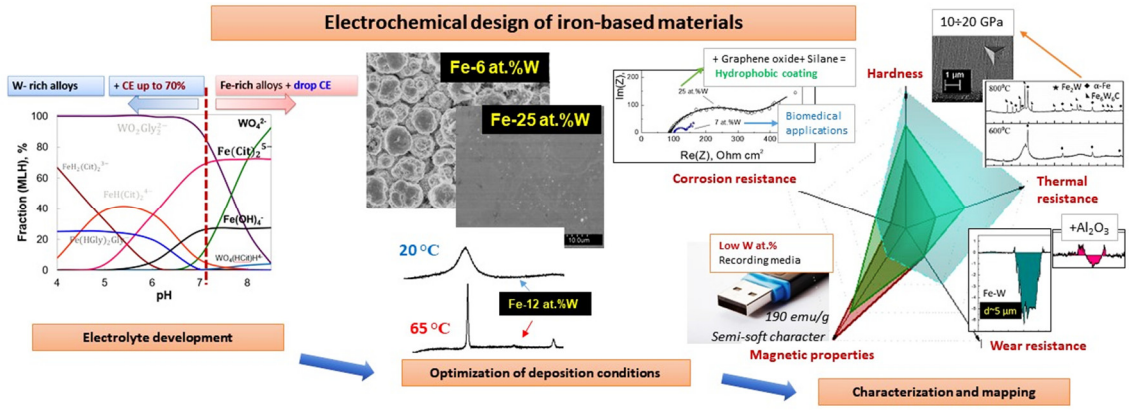

Figure 5. The outline on the electrochemical design of Fe-W alloys: from bath elaboration towards characterization and application.

One of the main factors impacting the mechanical, magnetic, catalytic, and tribological properties of Fe-alloys is linked to the nanocrystalline structure of electrodeposited materials obtained from complexing solutions. Moreover, the electrosynthesis of nanocrystalline alloys can be facilitated and optimized by applying thermodynamic approaches. Namely, the knowledge of the

 doi:10.20944/preprints202412.0663.v1

complex speciation (**Figure 5**) in the solutions can help to: (a) define the compositional stability ranges of electrodepositing baths, (b) correct Pourbaix diagrams for particular conditions, (c) find the codeposition conditions and ways for process intensification, (d) understand the influence of the composition of the bath on the composition and structure of electrodeposited alloys.

This interplay between parameters of electrochemical design is an opportunity to tailor such materials for versatile applications. which can be further enhanced by exploring the potential of micro- and nano-electrodeposits. [165]. Namely, excellent mechanical properties and thermal resistance of rich-W iron alloys can be explored for fusion reactors or other applications requiring thermal resistance. The soft magnetic character of Fe-rich alloys coupled with electrical properties, magnetostriction, and biocompatibility can be explored for micro-transformers, sensors, and NEMS fabrication respectively. Mechanical properties and advanced biodegradability of iron-based scaffolds show potential for bone tissue engineering.

To adopt these alloys for tribological applications the lubricated conditions should be applied to prevent the corrosion of iron-base alloys or to produce composites with the addition of inert hard particles such as Al_2O_3 or TiO_2 and others. The alternative way to increase the mechanical robustness and wear resistance of electrodeposited materials is carburization, where the thermal decomposition of ethanol in an inert gas atmosphere and at high temperatures is used to create carbide phases such as e.g., Fe_3W_3C [166]. These phases as we discussed earlier essentially contribute to increased hardness. Furthermore, for targeted applications, the corrosion resistance can be also amplified by increasing the hydrophobicity of Fe-W alloys by forming silane cross-linked graphene oxide and hydrophobic organosilane layers on top of the base material (**Figure 5**). The catalytic properties can also benefit from the formation of nanostructured electrodeposits (e.g., Ni-Fe nanosheets) that can be rationalized afterward by W-doping [167]. Furthermore, electrodeposited NiFeW hydroxide electrocatalysts for efficient water oxidation can outperform conventional 20 wt% Ir/C electrocatalysts [168].

Moreover, taking into account the growing focus on sustainability worldwide, synthesizing and discovering new applications for earth-abundant materials will increase. However, iron-based alloys that incorporate rare metals like Pt and palladium Pd demonstrate superior catalytic activity and stability compared to other alternatives. In this perspective, Pd-Fe and Pt-Fe materials are demonstrating their versatility as catalytic systems. Their chemo-physical properties can be easily adjusted by altering the synthetic parameters. It is essential to choose the appropriate system, as the selection depends on the active phase needed for a specific reaction [169].

A sustainable method for obtaining the mentioned materials could involve conducting galvanic replacement reactions on iron or iron alloys using solutions that contain platinum or palladium derived from their waste-leaching processes. Thus, research has demonstrated the effectiveness of the galvanic replacement method for producing catalysts based on a Fe-Zn substrate [170]. However, substantial effort is still needed to fully understand and implement eco-friendly electrochemical recovery of such materials.

Author Contributions: Conceptualization, NT and HC; writing—original draft preparation, NT, HC, and OB; writing—review and editing, HC and NT; illustration - NT. All authors have read and agreed to the published version of the manuscript.

Funding: This study was partially funded by the Research Council of Lithuania grant No. S-MIP-24-11, the Moldavian National project ANCD project 011204, and the European Union MSCA4Ukraine project, no. 1233494.

Acknowledgments: The authors are thankful to all partners of the H2020 “SELECTA” and “SMARTELECTRODES” projects for the fruitful collaboration on accomplished research.

Conflicts of Interest: The authors declare no conflicts of interest.

References

1. Our Common Future, Chapter 2: Towards Sustainable Development. UN Documents Gathering a Body of Global Agreements. Available Online: Http://Www.Un-Documents.Net/Ocf-02.Htm (Accessed on 11.07.2024).

2. Fajardo, A.S.; Westerhoff, P.; Sanchez-Sanchez, C.M.; Garcia-Segura, S. Earth-Abundant Elements a Sustainable Solution for Electrocatalytic Reduction of Nitrate. *Applied Catalysis B: Environmental* **2021**, *281*, 119465, doi:10.1016/j.apcatb.2020.119465.
3. Chirik, P.J.; Engle, K.M.; Simmons, E.M.; Wisniewski, S.R. Collaboration as a Key to Advance Capabilities for Earth-Abundant Metal Catalysis. *Org. Process Res. Dev.* **2023**, *27*, 1160–1184, doi:10.1021/acs.oprd.3c00025.
4. Bhatt, G.; Ghatak, A.; Murugavel, R. Futuristic Storage Devices: Single Molecular Magnets of Rare Earths versus Spin Crossover Systems of Earth-Abundant Metals. *J Chem Sci* **2023**, *135*, 40, doi:10.1007/s12039-023-02163-4.
5. Cardoso, R.M.F.; Esteves Da Silva, J.C.G.; Pinto Da Silva, L. Application of Engineered Nanomaterials as Nanocatalysts in Catalytic Ozonation: A Review. *Materials* **2024**, *17*, 3185, doi:10.3390/ma17133185.
6. Docherty, J.H.; Peng, J.; Dominey, A.P.; Thomas, S.P. Activation and Discovery of Earth-Abundant Metal Catalysts Using Sodium Tert-Butoxide. *Nature Chem* **2017**, *9*, 595–600, doi:10.1038/nchem.2697.
7. Gąsior, G.; Szczepański, J.; Radtke, A. Biodegradable Iron-Based Materials—What Was Done and What More Can Be Done? *Materials* **2021**, *14*, 3381, doi:10.3390/ma14123381.
8. Mostavan, A.; Paternoster, C.; Tolouei, R.; Ghali, E.; Dubé, D.; Mantovani, D. Effect of Electrolyte Composition and Deposition Current for Fe/Fe-P Electroformed Bilayers for Biodegradable Metallic Medical Applications. *Materials Science and Engineering: C* **2017**, *70*, 195–206, doi:10.1016/j.msec.2016.08.026.
9. Huang, T.; Cheng, J.; Bian, D.; Zheng, Y. Fe–Au and Fe–Ag Composites as Candidates for Biodegradable Stent Materials. *J Biomed Mater Res* **2016**, *104*, 225–240, doi:10.1002/jbm.b.33389.
10. Akbarzadeh, R.; Ghaedi, M.; Nasiri Kokhdan, S.; Jannesar, R.; Sadeghfar, F.; Sadri, F.; Tayebi, L. Electrochemical Hydrogen Storage, Photocatalytical and Antibacterial Activity of Fe Ag Bimetallic Nanoparticles Supported on TiO2 Nanowires. *International Journal of Hydrogen Energy* **2018**, *43*, 18316–18329, doi:10.1016/j.ijhydene.2018.07.175.
11. Sun, Y.; Zangari, G. Rational Compositional Control of Electrodeposited Ag–Fe Films. *Inorg. Chem.* **2020**, *59*, 5405–5417, doi:10.1021/acs.inorgchem.9b03600.
12. Mažeika, K.; Reklaitis, J.; Nicolenco, A.; Vainoris, M.; Tsyntsaru, N.; Cesiulis, H. Magnetic State Instability of Disordered Electrodeposited Nanogranular Fe Films. *Journal of Magnetism and Magnetic Materials* **2021**, *540*, 168433, doi:10.1016/j.jmmm.2021.168433.
13. Khazi, I.; Mescheder, U. Micromechanical Properties of Anomalously Electrodeposited Nanocrystalline Nickel-Cobalt Alloys: A Review. *Mater. Res. Express* **2019**, *6*, 082001, doi:10.1088/2053-1591/ab1bb0.
14. Torabinejad, V.; Aliofkhazraei, M.; Sabour Rouhaghdam, A.; Allahyarzadeh, M.H. Tribological Behavior of Electrodeposited Ni-Fe Multilayer Coating. *Tribology Transactions* **2017**, *60*, 923–931, doi:10.1080/10402004.2016.1230687.
15. Gamburg, Y.D.; Zangari, G. *Theory and Practice of Metal Electrodeposition*; Springer New York: New York, NY, 2011; ISBN 978-1-4419-9668-8.
16. Shojaei, Z.; Khayati, G.R.; Darezereshki, E. Review of Electrodeposition Methods for the Preparation of High-Entropy Alloys. *Int J Miner Metall Mater* **2022**, *29*, 1683–1696, doi:10.1007/s12613-022-2439-y.
17. Zangari, G. Electrodeposition of Alloys and Compounds in the Era of Microelectronics and Energy Conversion Technology. *Coatings* **2015**, *5*, 195–218, doi:10.3390/coatings5020195.
18. Bertero, E.; Manzano, C.V.; Pellicer, E.; Sort, J.; Ulfig, R.M.; Mischler, S.; Michler, J.; Philippe, L. 'Green' Cr(III)–Glycine Electrolyte for the Production of FeCrNi Coatings: Electrodeposition Mechanisms and Role of by-Products in Terms of Coating Composition and Microstructure. *RSC Adv.* **2019**, *9*, 25762–25775, doi:10.1039/C9RA04262H.
19. Białostocka, A.M.; Klekotka, M.; Klekotka, U.; Kalska-Szostko, B. Tribological Properties of the FeNi Alloys Electrodepositedwith and without External Magnetic Field Assistance. *Eksploatacja i Niezawodność – Maintenance and Reliability* **2022**, *24*, 687–694, doi:10.17531/ein.2022.4.9.
20. Schlesinger, M. *Modern Electroplating*; The ECS series of texts and monographs; 5th ed.; Wiley: Hoboken, 2011; ISBN 978-0-470-16778-6.
21. Gonçalves, S.; Andrade, V.; Sousa, C.T.; Araújo, J.P.; Belo, J.H.; Apolinário, A. Tunable Iron–Cobalt Thin Films Grown by Electrodeposition. *Magnetochemistry* **2023**, *9*, 161, doi:10.3390/magnetochemistry9070161.
22. Ying, Y.; Wang, H.; Zheng, J.; Yu, J.; Li, W.; Qiao, L.; Cai, W.; Che, S. Preparation, Microstructure, and Magnetic Properties of Electrodeposited Nanocrystalline L10 FePt Films. *J Supercond Nov Magn* **2020**, *33*, 3563–3570, doi:10.1007/s10948-020-05624-w.
23. Annamalai, S.; Chelvane, A.J.; Mohanty, J. Enhancement of Magnetic and Surface Properties in Magneto-Pulse Electrodeposited Fe-Pd Alloy Thin Films at Various Deposition Potentials. *Mater. Res. Express* **2019**, *6*, 066110, doi:10.1088/2053-1591/ab0bc6.
24. Rezaei, M.; Haghshenas, D.F.; Ghorbani, M.; Dolati, A. Electrochemical Behavior of Nanostructured Fe-Pd Alloy During Electrodeposition on Different Substrates. *J. Electrochem. Sci. Technol* **2018**, *9*, 202–211, doi:10.33961/JECST.2018.9.3.202.

25. Nicolenco, A.; Gómez, A.; Chen, X.-Z.; Menéndez, E.; Fornell, J.; Pané, S.; Pellicer, E.; Sort, J. Strain Gradient Mediated Magnetoelectricity in Fe-Ga/P(VDF-TrFE) Multiferroic Bilayers Integrated on Silicon. *Applied Materials Today* **2020**, *19*, 100579, doi:10.1016/j.apmt.2020.100579.
26. Nicolenco, A.; Chen, Y.; Tsyntsaru, N.; Cesiulis, H.; Pellicer, E.; Sort, J. Mechanical, Magnetic and Magnetostrictive Properties of Porous Fe-Ga Films Prepared by Electrodeposition. *Materials & Design* **2021**, *208*, 109915, doi:10.1016/j.matdes.2021.109915.
27. Tsyntsaru, N.; Cesiulis, H.; Donten, M.; Sort, J.; Pellicer, E.; Podlaha-Murphy, E.J. Modern Trends in Tungsten Alloys Electrodeposition with Iron Group Metals. *Surf. Engin. Appl.Electrochem.* **2012**, *48*, 491–520, doi:10.3103/S1068375512060038.
28. Mukhtar, A.; Wu, K. Coupled Electrodeposition and Magnetic Properties of Ternary CoFeW Alloys. *Materials Characterization* **2022**, *192*, 112246, doi:10.1016/j.matchar.2022.112246.
29. Nicolenco, A.; Tsyntsaru, N.; Fornell, J.; Pellicer, E.; Reklaitis, J.; Baltrunas, D.; Cesiulis, H.; Sort, J. Mapping of Magnetic and Mechanical Properties of Fe-W Alloys Electrodeposited from Fe(III)-Based Glycolate-Citrate Bath. *Materials & Design* **2018**, *139*, 429–438, doi:10.1016/j.matdes.2017.11.011.
30. Ghaferi, Z.; Sharafi, S.; Bahrololoom, M.E. The Role of Electrolyte pH on Phase Evolution and Magnetic Properties of CoFeW Codeposited Films. *Applied Surface Science* **2016**, *375*, 35–41, doi:10.1016/j.apsusc.2016.03.063.
31. Yermolenko, I.Yu.; Ved', M.V.; Sakhnenko, N.D.; Shipkova, I.G.; Zyubanova, S.I. Nanostructured Magnetic Films Based on Iron with Refractory Metals. *Journal of Magnetism and Magnetic Materials* **2019**, *475*, 115–120, doi:10.1016/j.jmmm.2018.11.104.
32. Cirovic, N.; Spasojevic, P.; Ribic-Zelenovic, L.; Maskovic, P.; Spasojevic, M. Synthesis, Structure and Properties of Nickel-Iron-Tungsten Alloy Electrodeposits - Part I: Effect of Synthesis Parameters on Chemical Composition, Microstructure and Morphology. *Sci Sintering* **2015**, *47*, 347–365, doi:10.2298/SOS1503347C.
33. Cirovic, N.; Spasojevic, P.; Ribic-Zelenovic, L.; Maskovic, P.; Maricic, A.; Spasojevic, M. Synthesis, Structure and Properties of Nickel-Iron-Tungsten Alloy Electrodeposits - Part II: Effect of Microstructure on Hardness, Electrical and Magnetic Properties. *Sci Sintering* **2016**, *48*, 1–16, doi:10.2298/SOS1601001C.
34. Candidate List of Substances of Very High Concern for Authorisation. Available Online Https://Echa.Europa.Eu/Candidate-List-Table?p_p_id=disslists_WAR_disslistsportlet&p_p_lifecycle=1&p_p_state=normal&p_p_mode=view&p_p_col_id=column-1&p_p_col_pos=2&p_p_col_count=3&_disslists_WAR_disslistsportlet_javax.Portlet.action=searchDissListsNo. Accessed on 11.05.2024.
35. Mrkonjić Zajkoska, S.; Dobročka, E.; Hansal, S.; Mann, R.; Hansal, W.E.G.; Kautek, W. Tartrate-Based Electrolyte for Electrodeposition of Fe–Sn Alloys. *Coatings* **2019**, *9*, 313, doi:10.3390/coatings9050313.
36. Zajkoska, S.M.; Mann, R.; Hansal, W.; Roy, S.; Kautek, W. Electrodeposition of Fe-Sn from the Chloride-Based Electrolyte. *Transactions of the IMF* **2019**, *97*, 247–253, doi:10.1080/00202967.2019.1647670.
37. Giefers, H.; Nicol, M. High Pressure X-Ray Diffraction Study of All Fe–Sn Intermetallic Compounds and One Fe–Sn Solid Solution. *Journal of Alloys and Compounds* **2006**, *422*, 132–144, doi:10.1016/j.jallcom.2005.11.061.
38. García-Arribas, A.; Fdez-Gubieda, M.L.; Barandiarán, J.M. Comparative Study of the Structure and Magnetic Properties of Co-P and Fe-P Amorphous Alloys. *Phys. Rev. B* **2000**, *61*, 6238–6245, doi:10.1103/PhysRevB.61.6238.
39. Liu, T.; Ji, B.; Wu, Y.; Liu, Z.; Wang, W. Effects of the pH Value on the Electrodeposition of Fe–P Alloy as a Magnetic Film Material. *J. Phys. Chem. C* **2022**, *126*, 15472–15484, doi:10.1021/acs.jpcc.2c04176.
40. Kovalska, N.; Tsyntsaru, N.; Cesiulis, H.; Gebert, A.; Fornell, J.; Pellicer, E.; Sort, J.; Hansal, W.; Kautek, W. Electrodeposition of Nanocrystalline Fe-P Coatings: Influence of Bath Temperature and Glycine Concentration on Structure, Mechanical and Corrosion Behavior. *Coatings* **2019**, *9*, 189, doi:10.3390/coatings9030189.
41. Kovalska, N.; Hansal, W.E.G.; Tsyntsaru, N.; Cesiulis, H.; Gebert, A.; Kautek, W. Electrodeposition and Corrosion Behaviour of Nanocrystalline Fe–P Coatings. *Transactions of the IMF* **2019**, *97*, 89–94, doi:10.1080/00202967.2019.1578130.
42. Naor, A.; Eliaz, N.; Gileadi, E. Electrodeposition of Alloys of Rhenium with Iron-Group Metals from Aqueous Solutions. *ECS Trans.* **2010**, *25*, 137–149, doi:10.1149/1.3327232.
43. Li, X.; Chen, Y.; Zheng, X.; Zhu, Y.; Wang, Z.; Wang, Y. One-Step Electrodeposition of Composition-Controllable Dendritic NiFe Alloy Electrocatalysts for Oxygen Evolution Reaction. *Journal of Alloys and Compounds* **2023**, *968*, 172313, doi:10.1016/j.jallcom.2023.172313.
44. Xiong, Y.; He, P. A Review on Electrocatalysis for Alkaline Oxygen Evolution Reaction (OER) by Fe-Based Catalysts. *J Mater Sci* **2023**, doi:10.1007/s10853-023-08176-1.
45. Kutyła, D.; Skibińska, K.; Wojtysiak, M.; Salci, A.; Kołczyk-Siedlecka, K.; Wojtaszek, K.; Wojnicki, M.; Żabiński, P.; Solmaz, R. Electrochemical Preparation and Alkaline Water Splitting Activity of Ternary Co–

Fe–Mo Non-Crystalline Coatings. *International Journal of Hydrogen Energy* **2024**, *51*, 1450–1459, doi:10.1016/j.ijhydene.2023.07.333.
46. Ni, R.; Xu, W.; Wang, C.; Man, Z.; Cheng, X. The Application of Iron-Manganese Compounds towards Micropollutants Purification in Water: A Critical Review. *Chemical Engineering Journal* **2024**, *493*, 152553, doi:10.1016/j.cej.2024.152553.
47. Xia, Q.; Jiang, Z.; Wang, J.; Yao, Z. A Facile Preparation of Hierarchical Dendritic Zero-Valent Iron for Fenton-like Degradation of Phenol. *Catalysis Communications* **2017**, *100*, 57–61, doi:10.1016/j.catcom.2017.06.017.
48. Vainoris, M.; Nicolenco, A.; Tsyntsaru, N.; Podlaha-Murphy, E.; Alcaide, F.; Cesiulis, H. Electrodeposited Fe on Cu Foam as Advanced Fenton Reagent for Catalytic Mineralization of Methyl Orange. *Front. Chem.* **2022**, *10*, 977980, doi:10.3389/fchem.2022.977980.
49. Theofanidis, S.A.; Galvita, V.V.; Konstantopoulos, C.; Poelman, H.; Marin, G.B. Fe-Based Nano-Materials in Catalysis. *Materials* **2018**, *11*, 831, doi:10.3390/ma11050831.
50. Protsenko, V.S.; Danilov, F.I. Current Trends in Electrodeposition of Electrocatalytic Coatings. In *Methods for Electrocatalysis*; Inamuddin, Boddula, R., Asiri, A.M., Eds.; Springer International Publishing: Cham, 2020; pp. 263–299 ISBN 978-3-030-27160-2.
51. Mulone, A.; Nicolenco, A.; Imaz, N.; Fornell, J.; Sort, J.; Klement, U. Effect of Heat Treatments on the Mechanical and Tribological Properties of Electrodeposited Fe–W/Al2O3 Composites. *Wear* **2020**, *448–449*, 203232, doi:10.1016/j.wear.2020.203232.
52. Nicolenco, A.; Mulone, A.; Imaz, N.; Tsyntsaru, N.; Sort, J.; Pellicer, E.; Klement, U.; Cesiulis, H.; García-Lecina, E. Nanocrystalline Electrodeposited Fe-W/Al2O3 Composites: Effect of Alumina Sub-Microparticles on the Mechanical, Tribological, and Corrosion Properties. *Front. Chem.* **2019**, *7*, 241, doi:10.3389/fchem.2019.00241.
53. Starosta, R.; Zielinski, A. Effect of Chemical Composition on Corrosion and Wear Behaviour of the Composite Ni–Fe–Al2O3 Coatings. *Journal of Materials Processing Technology* **2004**, *157–158*, 434–441, doi:10.1016/j.jmatprotec.2004.09.068.
54. Jin, H.; Ji, R.; Dong, T.; Liu, S.; Zhang, F.; Zhao, L.; Ma, C.; Cai, B.; Liu, Y. Efficient Fabrication and Characterization of Ni-Fe-WC Composite Coatings with High Corrosion Resistance. *Journal of Materials Research and Technology* **2022**, *16*, 152–167, doi:10.1016/j.jmrt.2021.11.145.
55. Tsyntsaru, N.; Cesiulis, H.; Budreika, A.; Ye, X.; Juskenas, R.; Celis, J.-P. The Effect of Electrodeposition Conditions and Post-Annealing on Nanostructure of Co–W Coatings. *Surface and Coatings Technology* **2012**, *206*, 4262–4269, doi:10.1016/j.surfcoat.2012.04.036.
56. Tsyntsaru, N.; Bobanova, J.; Ye, X.; Cesiulis, H.; Dikusar, A.; Prosycevas, I.; Celis, J.-P. Iron–Tungsten Alloys Electrodeposited under Direct Current from Citrate–Ammonia Plating Baths. *Surface and Coatings Technology* **2009**, *203*, 3136–3141, doi:10.1016/j.surfcoat.2009.03.041.
57. Wang, S.; Zeng, C.; Ling, Y.; Wang, J.; Xu, G. Phase Transformations and Electrochemical Characterizations of Electrodeposited Amorphous Fe–W Coatings. *Surface and Coatings Technology* **2016**, *286*, 36–41, doi:10.1016/j.surfcoat.2015.12.011.
58. Wodarz, S.; Hashimoto, S.; Kambe, M.; Zangari, G.; Homma, T. Templated Electrochemical Synthesis of Fe–Pt Nanopatterns for High-Density Memory Applications. *ACS Appl. Nano Mater.* **2018**, *1*, 2317–2323, doi:10.1021/acsanm.8b00391.
59. Eliaz, N.; Gileadi, E. Induced Codeposition of Alloys of Tungsten, Molybdenum and Rhenium with Transition Metals. In *Modern Aspects of Electrochemistry*; Vayenas, C.G., White, R.E., Gamboa-Aldeco, M.E., Eds.; Modern Aspects of Electrochemistry; Springer New York: New York, NY, 2008; Vol. 42, pp. 191–301 ISBN 978-0-387-49488-3.
60. Li, X. Electrodeposition of Multi-Component Alloys: Thermodynamics, Kinetics and Mechanism. *Current Opinion in Electrochemistry* **2023**, *39*, 101289, doi:10.1016/j.coelec.2023.101289.
61. Survila, A. Electrochemistry of Metal Complexes: Applications from Electroplating to Oxide Layer Formation; 1. Auflage.; Wiley-VCH: Weinheim, Germany, 2015; ISBN 978-3-527-69125-8.
62. Heusler, K.E. Multicomponent Electrodes. *Electrochimica Acta* **1996**, *41*, 411–418, doi:10.1016/0013-4686(95)00321-5.
63. Nicolenco, A.; Tsyntsaru, N.; Cesiulis, H. Fe (III)-Based Ammonia-Free Bath for Electrodeposition of Fe-W Alloys. *J. Electrochem. Soc.* **2017**, *164*, D590–D596, doi:10.1149/2.1001709jes.
64. Mulone, A.; Nicolenco, A.; Imaz, N.; Martinez-Nogues, V.; Tsyntsaru, N.; Cesiulis, H.; Klement, U. Improvement in the Wear Resistance under Dry Friction of Electrodeposited Fe-W Coatings through Heat Treatments. *Coatings* **2019**, *9*, 66, doi:10.3390/coatings9020066.
65. Cesiulis, H.; Baltutiene, A.; Donten, M.; Donten, M.; Stojek, Z. Increase in Rate of Electrodeposition and in Ni(II) Concentration in the Bath as a Way to Control Grain Size of Amorphous/Nanocrystalline Ni-W Alloys. *J Solid State Electrochem* **2002**, *6*, 237–244, doi:10.1007/s100080100225.

66. Kovalska, N.; Pfaffeneder-Kmen, M.; Tsyntsaru, N.; Mann, R.; Henrikas Cesiulis; Hansal, W.; Kautek, W. The Role of Glycine in the Iron-Phosphorous Alloy Electrodeposition. *Electrochimica Acta* **2019**, *309*, 450–459, doi:10.1016/j.electacta.2019.03.203.
67. Mehrizi, S.; Sohi, M.H.; Saremi, M. Effect of Sodium Citrate as Complexing on Electrochemical Behavior and Speciation Diagrams of CoFeNiCu Baths. *Ionics* **2013**, *19*, 911–918, doi:10.1007/s11581-012-0815-8.
68. Fortas, G.; Ouir, S.; Manseri, A.; Djerir, W.; Smaili, F.; Gabouze, N.; Haine, N. Influence of Deposition Parameters on the Electrodeposited Ternary CoFeCu Coatings. *J Mater Sci: Mater Electron* **2024**, *35*, 1462, doi:10.1007/s10854-024-13103-4.
69. Singh, A.K.; Zhou, L.; Shinde, A.; Suram, S.K.; Montoya, J.H.; Winston, D.; Gregoire, J.M.; Persson, K.A. Electrochemical Stability of Metastable Materials. *Chem. Mater.* **2017**, *29*, 10159–10167, doi:10.1021/acs.chemmater.7b03980.
70. Brenner, A. *Electrodeposition of Alloys: Principles and Practice*; Academic Press: New York, 1963; ISBN 978-1-4832-2311-7.
71. Podlaha, E.J.; Landolt, D. Induced Codeposition: I. An Experimental Investigation of Ni-Mo Alloys. *J. Electrochem. Soc.* **1996**, *143*, 885–892, doi:10.1149/1.1836553.
72. Zech, N.; Podlaha, E.J.; Landolt, D. Anomalous Codeposition of Iron Group Metals: I. Experimental Results. *J. Electrochem. Soc.* **1999**, *146*, 2886–2891, doi:10.1149/1.1392024.
73. V. P. Greco Rhenium Alloys - Iron Group Metals (Electrodeposition and Properties); 1971;
74. Zhulikov, V.V.; Gamburg, Yu.D. Electrodeposition of Rhenium and Its Alloys. *Russ J Electrochem* **2016**, *52*, 847–857, doi:10.1134/S102319351609010X.
75. Electrochemical Series. In *Corrosion: Materials*; Cramer, S.D., Covino, B.S., Eds.; ASM International, 2005; pp. 665–671 ISBN 978-1-62708-183-2.
76. Vajo, J.J.; Aikens, D.A.; Ashley, L.; Poeltl, D.E.; Bailey, R.A.; Clark, H.M.; Bunce, S.C. Facile Electroreduction of Perrhenate in Weakly Acidic Citrate and Oxalate Media. *Inorg. Chem.* **1981**, *20*, 3328–3333, doi:10.1021/ic50224a037.
77. Contu, F.; Taylor, S.R. Further Insight into the Mechanism of Re–Ni Electrodeposition from Concentrated Aqueous Citrate Baths. *Electrochimica Acta* **2012**, *70*, 34–41, doi:10.1016/j.electacta.2012.03.010.
78. Vargas-Uscategui, A.; Mosquera, E.; Cifuentes, L. Analysis of the Electrodeposition Process of Rhenium and Rhenium Oxides in Alkaline Aqueous Electrolyte. *Electrochimica Acta* **2013**, *109*, 283–290, doi:10.1016/j.electacta.2013.07.091.
79. Baranov, S.A.; Dikusar, A.I. Kinetics of Electrochemical Nanonucleation during Induced Codeposition of Iron-Group Metals with Refractory Metals (W, Mo, Re). *Surf. Engin. Appl.Electrochem.* **2022**, *58*, 429–439, doi:10.3103/S1068375522050027.
80. Torabinejad, V.; Aliofkhazraei, M.; Assareh, S.; Allahyarzadeh, M.H.; Rouhaghdam, A.S. Electrodeposition of Ni-Fe Alloys, Composites, and Nano Coatings–A Review. *Journal of Alloys and Compounds* **2017**, *691*, 841–859, doi:10.1016/j.jallcom.2016.08.329.
81. Park, D.-Y.; Yoo, B.Y.; Kelcher, S.; Myung, N.V. Electrodeposition of Low-Stress High Magnetic Moment Fe-Rich FeCoNi Thin Films. *Electrochimica Acta* **2006**, *51*, 2523–2530, doi:10.1016/j.electacta.2005.07.037.
82. Arai, S.; Tomiita, K.; Shimizu, M.; Narita, H. Electrodeposition of Fe-Ni Alloy Films Having Invar Compositions with Fe^{3+} as the Sole Iron Source. *J. Electrochem. Soc.* **2023**, *170*, 112506, doi:10.1149/1945-7111/ad0dc5.
83. Liang, D.; Mallett, J.J.; Zangari, G. Electrodeposition of Fe–Pt Films with Low Oxide Content Using an Alkaline Complexing Electrolyte. *ACS Appl. Mater. Interfaces* **2010**, *2*, 961–964, doi:10.1021/am100066x.
84. Liang, D.; Zangari, G. Fe–Pt Magnetic Multilayers by Electrochemical Deposition. *Electrochimica Acta* **2011**, *56*, 10567–10574, doi:10.1016/j.electacta.2011.01.085.
85. Yar-Mukhamedova, G.; Ved, M.; Sakhnenko, N.; Karakurkchi, A.; Yermolenko, I. Iron Binary and Ternary Coatings with Molybdenum and Tungsten. *Applied Surface Science* **2016**, *383*, 346–352, doi:10.1016/j.apsusc.2016.04.046.
86. Ramaprakash, M.; Jerom Samraj, A.; Neelavannan, M.G.; Rajasekaran, N. The Induced Co-Deposition of Ni–Mo–W Ternary Alloy; Coatings for Hardness and Corrosion Resistance Applications. *Results in Surfaces and Interfaces* **2024**, *15*, 100235, doi:10.1016/j.rsurfi.2024.100235.
87. He, F.; Yang, J.; Lei, T.; Gu, C. Structure and Properties of Electrodeposited Fe–Ni–W Alloys with Different Levels of Tungsten Content: A Comparative Study. *Applied Surface Science* **2007**, *253*, 7591–7598, doi:10.1016/j.apsusc.2007.03.068.
88. Wang, S.; Ling, Y.; Zhang, J.; Wang, J.; Xu, G. Microstructure and Properties of Hydrophobic Films Derived from Fe-W Amorphous Alloy. *Int J Miner Metall Mater* **2014**, *21*, 395–400, doi:10.1007/s12613-014-0921-x.
89. Dobrzańska-Danikiewicz, A.D.; Wolany, W. A Rhenium Review – from Discovery to Novel Applications. *Archives of Materials Science and Engineering* **2016**, *82*, 70–78, doi:10.5604/01.3001.0009.7106.
90. Jones, T. Rhenium Plating. *Metal Finishing* **2003**, *101*, 86–96, doi:10.1016/S0026-0576(03)80439-7.

91. Tsyntsaru, N.; Cesiulis, H.; Pellicer, E.; Celis, J.-P.; Sort, J. Structural, Magnetic, and Mechanical Properties of Electrodeposited Cobalt–Tungsten Alloys: Intrinsic and Extrinsic Interdependencies. *Electrochimica Acta* **2013**, *104*, 94–103, doi:10.1016/j.electacta.2013.04.022.
92. Sriraman, K.R.; Ganesh Sundara Raman, S.; Seshadri, S.K. Synthesis and Evaluation of Hardness and Sliding Wear Resistance of Electrodeposited Nanocrystalline Ni–W Alloys. *Materials Science and Engineering: A* **2006**, *418*, 303–311, doi:10.1016/j.msea.2005.11.046.
93. Haché, M.J.R.; Tam, J.; Erb, U.; Zou, Y. Electrodeposited NiFeCo-(Mo,W) High-Entropy Alloys with Nanocrystalline and Amorphous Structures. *Journal of Alloys and Compounds* **2023**, *952*, 170026, doi:10.1016/j.jallcom.2023.170026.
94. Vernickaite, E.; Tsyntsaru, N.; Sobczak, K.; Cesiulis, H. Electrodeposited Tungsten-Rich Ni-W, Co-W and Fe-W Cathodes for Efficient Hydrogen Evolution in Alkaline Medium. *Electrochimica Acta* **2019**, *318*, 597–606, doi:10.1016/j.electacta.2019.06.087.
95. Silkin, S.A.; Gotelyak, A.V.; Tsyntsaru, N.I.; Dikusar, A.I. Electrodeposition of Alloys of the Iron Group Metals with Tungsten from Citrate and Gluconate Solutions: Size Effect of Microhardness. *Surf. Engin. Appl.Electrochem.* **2017**, *53*, 7–14, doi:10.3103/S1068375517010136.
96. Belevskii, S.S.; Gotelyak, A.V.; Silkin, S.A.; Dikusar, A.I. Macroscopic Size Effect on the Microhardness of Electroplated Iron Group Metal—Tungsten Alloy Coatings: Impact of Electrode Potential and Oxygen-Containing Impurities. *Surf. Engin. Appl.Electrochem.* **2019**, *55*, 46–52, doi:10.3103/S1068375519010058.
97. Belevskii, S.S.; Danilchuk, V.V.; Gotelyak, A.V.; Lelis, M.; Yushchenko, S.P.; Dikusar, A.I. Electrodeposition of Fe–W Alloys from Citrate Bath: Impact of Anode Material. *Surf. Engin. Appl.Electrochem.* **2020**, *56*, 1–12, doi:10.3103/S1068375520010020.
98. Myrzak, V.; Gotelyak, A.V.; Dikusar, A.I. Size Effects in the Surface Properties of Electroplated Alloys between Iron Group Metals and Tungsten. *Surf. Engin. Appl.Electrochem.* **2021**, *57*, 409–418, doi:10.3103/S1068375521040128.
99. Gamburg, Yu.D.; Zakharov, E.N. Electrodeposition of Ternary Fe–W–H Alloys. *Surf. Engin. Appl.Electrochem.* **2019**, *55*, 402–409, doi:10.3103/S1068375519040033.
100. Belevskii, S.S.; Bobanova, Zh.I.; Buravets, V.A.; Gotelyak, A.V.; Danil'chuk, V.V.; Silkin, S.A.; Dikusar, A.I. Electrodeposition of Co–W Coatings from Boron Gluconate Electrolyte with a Soluble Tungsten Anode. *Russ J Appl Chem* **2016**, *89*, 1427–1433, doi:10.1134/S107042721609007X.
101. Ledwig, P.; Kac, M.; Kopia, A.; Falkus, J.; Dubiel, B. Microstructure and Properties of Electrodeposited Nanocrystalline Ni-Co-Fe Coatings. *Materials* **2021**, *14*, 3886, doi:10.3390/ma14143886.
102. Chou, M.-C.; Chu, C.-F.; Wu, S.-T. Phase Transformations of Electroplated Amorphous Iron–Tungsten–Carbon Film. *Materials Chemistry and Physics* **2003**, *78*, 59–66, doi:10.1016/S0254-0584(02)00217-1.
103. Mulone, A.; Nicolenco, A.; Hoffmann, V.; Klement, U.; Tsyntsaru, N.; Cesiulis, H. In-Depth Characterization of as-Deposited and Annealed Fe-W Coatings Electrodeposited from Glycolate-Citrate Plating Bath. *Electrochimica Acta* **2018**, *261*, 167–177, doi:10.1016/j.electacta.2017.12.051.
104. Park, J.-H.; Kim, J.-I.; Shinohara, Y.; Hagio, T.; Umehara, N.; Ichino, R. Super Hardening of Fe W Alloy Plating by Phase Transformation of Amorphous to Metal Carbides-Dispersed Nanocrystalline Alloys and Application as Promising Alternative for Hard Chromium Plating. *Surface and Coatings Technology* **2024**, *477*, 130388, doi:10.1016/j.surfcoat.2024.130388.
105. Köse, M.; Tan, S.; Algül, H.; Alp, A.; Akbulut, H.; Uysal, M. Effect of Different Heat Treatment Temperatures on Fe W Alloy Electrodeposits: Tribological and Electrochemical Analysis. *Surface and Coatings Technology* **2024**, *485*, 130852, doi:10.1016/j.surfcoat.2024.130852.
106. Marvel, C.J.; Cantwell, P.R.; Harmer, M.P. The Critical Influence of Carbon on the Thermal Stability of Nanocrystalline Ni–W Alloys. *Scripta Materialia* **2015**, *96*, 45–48, doi:10.1016/j.scriptamat.2014.10.022.
107. Marvel, C.J.; Yin, D.; Cantwell, P.R.; Harmer, M.P. The Influence of Oxygen Contamination on the Thermal Stability and Hardness of Nanocrystalline Ni–W Alloys. *Materials Science and Engineering: A* **2016**, *664*, 49–57, doi:10.1016/j.msea.2016.03.129.
108. Mulone, A.; Nicolenco, A.; Fornell, J.; Pellicer, E.; Tsyntsaru, N.; Cesiulis, H.; Sort, J.; Klement, U. Enhanced Mechanical Properties and Microstructural Modifications in Electrodeposited Fe-W Alloys through Controlled Heat Treatments. *Surface and Coatings Technology* **2018**, *350*, 20–30, doi:10.1016/j.surfcoat.2018.07.007.
109. Herzer, G. Grain Size Dependence of Coercivity and Permeability in Nanocrystalline Ferromagnets. *IEEE Trans. Magn.* **1990**, *26*, 1397–1402, doi:10.1109/20.104389.
110. Zhang, Y.; Ivey, D.G. Electrodeposition of Nanocrystalline CoFe Soft Magnetic Thin Films from Citrate-Stabilized Baths. *Materials Chemistry and Physics* **2018**, *204*, 171–178, doi:10.1016/j.matchemphys.2017.10.043.
111. Spasojevic, M.; Plazinic, M.; Lukovic, M.; Maricic, A.; Spasojevic, M. The Effect of Annealing and Frequency of the External Magnetic Field on Magnetic Properties of Nanostructured Electrodeposit of the Ni86,0Fe9,8W1,3Cu2,9 Alloy. *Materials Chemistry and Physics* **2020**, *254*, 123513, doi:10.1016/j.matchemphys.2020.123513.

112. Mehrizi, S.; Molaei, M.J.; Sohi, M.H. An Investigation on Magnetic Properties and Electrical Resistivity of Nanocrystalline CoFeNi Thick Films Synthesized through Stabilized Bath. *Journal of Materials Research and Technology* **2022**, *21*, 2547–2554, doi:10.1016/j.jmrt.2022.10.002.
113. Hernández, S.C.; Yoo, B.Y.; Stefanescu, E.; Khizroev, S.; Myung, N.V. Electrodeposition of Iron–Palladium Thin Films. *Electrochimica Acta* **2008**, *53*, 5621–5627, doi:10.1016/j.electacta.2008.03.001.
114. Faltas, M.; Pillars, J.; Soule, L.; Meyerson, M.L.; Rodriguez, M.A.; Valdez, N.R.; Oglesby, S.; Jackson, N.; El-Kady, I. Electrodeposited NiFeCo + Tb and Dy for Enhanced Magnetostrictive Properties and Soft Magnetism. *Thin Solid Films* **2024**, *800*, 140396, doi:10.1016/j.tsf.2024.140396.
115. Wang, Q.; Li, M.; Weng, L.; Huang, W. Dual-Mode Sensing Based on Oriented Magnetostrictive Films by Electrodepositon. *IEEE Sensors J.* **2024**, *24*, 23667–23675, doi:10.1109/JSEN.2024.3412283.
116. Barbano, E.P.; Carlos, I.A.; Vallés, E. Electrochemical Synthesis of Fe-W and Fe-W-P Magnetic Amorphous Films and Fe-W Nanowires. *Surface and Coatings Technology* **2017**, *324*, 80–84, doi:10.1016/j.surfcoat.2017.05.071.
117. Ren, Q.Q.; Fan, J.L.; Han, Y.; Gong, H.R. Structural, Thermodynamic, Mechanical, and Magnetic Properties of FeW System. *Journal of Applied Physics* **2014**, *116*, 093909, doi:10.1063/1.4894396.
118. Mundotiya, B.M.; Dinulovic, D.; Rissing, L.; Wurz, M.C. Fabrication and Characterization of a Ni-Fe-W Core Microtransformer for High-Frequency Power Applications. *Sensors and Actuators A: Physical* **2017**, *267*, 42–47, doi:10.1016/j.sna.2017.09.032.
119. M., K.; H. B., R. Effect of Electrolytic Bath Temperature on Magnetic and Structural Properties of Electrodeposited Ni Fe W Nano Crystalline Thin Films. *Orient. J. Chem* **2017**, *33*, 2899–2904, doi:10.13005/ojc/330624.
120. Ved', M.; Yermolenko, I.; Sachanova, Yu.; Sakhnenko, N. Refractory Metals Influence on the Properties of Fe-Co-Mo(W) Electrolytic Alloys. *Materials Today: Proceedings* **2019**, *6*, 121–128, doi:10.1016/j.matpr.2018.10.084.
121. Kannan, R.; Ganesan, S.; Selvakumari, T.M. An Investigation on Effects of Annealing on Magnetic Properties of Ni-Fe-W-S Electrodeposited Coatings in Tri Sodium Citrate Bath. *Transaction A: Science* **2013**, *37*, doi:10.22099/ijsts.2013.1508.
122. Restriction Proposal on Chromium (VI) to Cover More Substances. Available Online. Https://Echa.Europa.Eu/-/Restriction-Proposal-on-Chromium-vi-to-Cover-More-Substances. Accessed on 12.09.2024.
123. Weston, D.P.; Harris, S.J.; Shipway, P.H.; Weston, N.J.; Yap, G.N. Establishing Relationships between Bath Chemistry, Electrodeposition and Microstructure of Co–W Alloy Coatings Produced from a Gluconate Bath. *Electrochimica Acta* **2010**, *55*, 5695–5708, doi:10.1016/j.electacta.2010.05.005.
124. Leyland, A.; Matthews, A. On the Significance of the H/E Ratio in Wear Control: A Nanocomposite Coating Approach to Optimised Tribological Behaviour. *Wear* **2000**, *246*, 1–11, doi:10.1016/S0043-1648(00)00488-9.
125. Rupert, T.J.; Schuh, C.A. Sliding Wear of Nanocrystalline Ni–W: Structural Evolution and the Apparent Breakdown of Archard Scaling. *Acta Materialia* **2010**, *58*, 4137–4148, doi:10.1016/j.actamat.2010.04.005.
126. Su, F.; Huang, P. Microstructure and Tribological Property of Nanocrystalline Co–W Alloy Coating Produced by Dual-Pulse Electrodeposition. *Materials Chemistry and Physics* **2012**, *134*, 350–359, doi:10.1016/j.matchemphys.2012.03.001.
127. Bobanova, Zh.I.; Dikusar, A.I.; Cesiulis, H.; Celis, J.-P.; Tsyntsaru, N.I.; Prosycevas, I. Micromechanical and Tribological Properties of Nanocrystalline Coatings of Iron-Tungsten Alloys Electrodeposited from Citrate-Ammonia Solutions. *Russ J Electrochem* **2009**, *45*, 895–901, doi:10.1134/S1023193509080096.
128. Park, J.-H.; Hagio, T.; Kamimoto, Y.; Ichino, R. The Effect of Bath pH on Electrodeposition and Corrosion Properties of Ternary Fe-W-Zn Alloy Platings. *J Solid State Electrochem* **2021**, *25*, 1901–1913, doi:10.1007/s10008-021-04964-4.
129. Zouch, F.; Antar, Z.; Bahri, A.; Elleuch, K.; Ürgen, M. Tribological Study of Fe–W–P Electrodeposited Coating on 316 L Stainless Steel. *Journal of Tribology* **2018**, *140*, 011301, doi:10.1115/1.4036628.
130. Tian, L.; Li, J.; Xing, H.; Yue, L.; Li, Z.; Wang, Y. Study of the Process of Preparing Amorphous Fe–W(La) Alloy Plating by Induced Co-Deposition. *mat express* **2023**, *13*, 1764–1771, doi:10.1166/mex.2023.2511.
131. Nicolenco, A.; Tsyntsaru, N.; Matijošius, T.; Asadauskas, S.; Cesiulis, H. WEAR RESISTANCE OF ELECTRODEPOSITED Fe-W ALLOY COATINGS UNDER DRY CONDITIONS AND IN THE PRESENCE OF RAPESEED OIL. *Green Tribology* **2018**, *1*, 16–23, doi:10.15544/greentribo.2018.04.
132. Bajwa, R.S.; Khan, Z.; Bakolas, V.; Braun, W. Water-Lubricated Ni-Based Composite (Ni–Al2O3, Ni–SiC and Ni–ZrO2) Thin Film Coatings for Industrial Applications. *Acta Metall. Sin. (Engl. Lett.)* **2016**, *29*, 8–16, doi:10.1007/s40195-015-0354-1.
133. Liang, J.; Wu, X.-W.; Ling, Y.; Yu, S.; Zhang, Z. Trilaminar Structure Hydrophobic Graphene Oxide Decorated Organosilane Composite Coatings for Corrosion Protection. *Surface and Coatings Technology* **2018**, *339*, 65–77, doi:10.1016/j.surfcoat.2018.02.002.
134. Vainoris, M.; Cesiulis, H.; Tsyntsaru, N. Metal Foam Electrode as a Cathode for Copper Electrowinning. *Coatings* **2020**, *10*, 822, doi:10.3390/coatings10090822.

135. Herraiz-Cardona, I.; Ortega, E.; Antón, J.G.; Pérez-Herranz, V. Assessment of the Roughness Factor Effect and the Intrinsic Catalytic Activity for Hydrogen Evolution Reaction on Ni-Based Electrodeposits. *International Journal of Hydrogen Energy* **2011**, *36*, 9428–9438, doi:10.1016/j.ijhydene.2011.05.047.
136. Vainoris, M.; Tsyntsaru, N.; Cesiulis, H. Modified Electrodeposited Cobalt Foam Coatings as Sensors for Detection of Free Chlorine in Water. *Coatings* **2019**, *9*, 306, doi:10.3390/coatings9050306.
137. Zhu, L.; Zhang, R.; Lv, W.; Wei, M.; Wang, W. One-Pot Hydrothermal Synthesis of Fe, W Co-Doped Ni3S2/NiS on Ni Foam for Bifunctional Oxygen Evolution and Urea Oxidation Reactions. *International Journal of Electrochemical Science* **2022**, *17*, 221043, doi:10.20964/2022.10.24.
138. Wang, S.; Yuan, D.; Sun, S.; Huang, S.; Wu, Y.; Zhang, L.; Dou, S.X.; Liu, H.K.; Dou, Y.; Xu, J. Iron, Tungsten Dual-Doped Nickel Sulfide as Efficient Bifunctional Catalyst for Overall Water Splitting. *Small* **2024**, 2311770, doi:10.1002/smll.202311770.
139. Č. Lačnjevac, M. M. Jaksic Synergetic Electrocatalytic Effects of D-Metals on the Hydrogen Evolution Reaction in Industrially Important Electrochemical Processes. *J. Res. Inst. Catalysis, Hokkaido Univ* **1983**, *31*, 7–33.
140. Tharamani, C.N.; Beera, P.; Jayaram, V.; Begum, N.S.; Mayanna, S.M. Studies on Electrodeposition of Fe–W Alloys for Fuel Cell Applications. *Applied Surface Science* **2006**, *253*, 2031–2037, doi:10.1016/j.apsusc.2006.03.077.
141. Bersirova, O.L.; Bilyk, S.V.; Kublanovs'kyi, V.S. Electrochemical Synthesis of Fe–W Nanostructural Electrocatalytic Coatings. *Mater Sci* **2018**, *53*, 732–738, doi:10.1007/s11003-018-0130-2.
142. Zhang, P.; Tan, W.; He, H.; Fu, Z. Binder-Free Quaternary Ni–Fe–W–Mo Alloy as a Highly Efficient Electrocatalyst for Oxygen Evolution Reaction. *Journal of Alloys and Compounds* **2021**, *853*, 157265, doi:10.1016/j.jallcom.2020.157265.
143. V. Bachvarov, M. Arnaudova, E. Lefterova, R. Rashkov Study of Oxygen Evolution Reaction on Iron Group-Based Electrodeposited Multicomponent Catalysts in Alkaline Media. Part i: Influence of the Composition. *Journal of Chemical Technology and Metallurgy* **2022**, *57*, 910–918.
144. Zhang, J.; Ling, Y.; Gao, W.; Wang, S.; Li, J. Enhanced Photoelectrochemical Water Splitting on Novel Nanoflake WO3 Electrodes by Dealloying of Amorphous Fe–W Alloys. *J. Mater. Chem. A* **2013**, *1*, 10677, doi:10.1039/c3ta12273e.
145. Ved', M.; Sakhnenko, N.; Nenastina, T.; Volobuyev, M.; Yermolenko, I. Corrosion and Mechanical Properties of Nanostructure Electrolytic Co-W and Fe-Co-W Alloys. *Materials Today: Proceedings* **2022**, *50*, 463–469, doi:10.1016/j.matpr.2021.11.293.
146. Stojić, D.Lj.; Cekić, B.D.; Maksić, A.D.; Kaninski, M.P.M.; Miljanić, Š.S. Intermetallics as Cathode Materials in the Electrolytic Hydrogen Production. *International Journal of Hydrogen Energy* **2005**, *30*, 21–28, doi:10.1016/j.ijhydene.2004.05.005.
147. Shen, Y.; Wu, P.; Wang, C.; Yuan, W.; Yang, W.; Shang, X. Electrodeposition of Amorphous Ni–Fe–Mo Composite as a Binder-Free and High-Performance Electrocatalyst for Hydrogen Generation from Alkaline Water Electrolysis. *International Journal of Hydrogen Energy* **2023**, *48*, 33130–33138, doi:10.1016/j.ijhydene.2023.03.327.
148. Zhou, D.; Li, P.; Xu, W.; Jawaid, S.; Mohammed-Ibrahim, J.; Liu, W.; Kuang, Y.; Sun, X. Recent Advances in Non-Precious Metal-Based Electrodes for Alkaline Water Electrolysis. *ChemNanoMat* **2020**, *6*, 336–355, doi:10.1002/cnma.202000010.
149. Vernickaitė, E.; Bersirova, O.; Cesiulis, H.; Tsyntsaru, N. Design of Highly Active Electrodes for Hydrogen Evolution Reaction Based on Mo-Rich Alloys Electrodeposited from Ammonium Acetate Bath. *Coatings* **2019**, *9*, 85, doi:10.3390/coatings9020085.
150. Huang, Y.; Wu, Y.; Zhang, Z.; Yang, L.; Zang, Q. Rapid Electrodeposited of Self-Supporting Ni-Fe-Mo Film on Ni Foam as Affordable Electrocatalysts for Oxygen Evolution Reaction. *Electrochimica Acta* **2021**, *390*, 138754, doi:10.1016/j.electacta.2021.138754.
151. Huang, X.; Liu, K.; Vrijburg, W.L.; Ouyang, X.; Iulian Dugulan, A.; Liu, Y.; Tiny Verhoeven, M.W.G.M.; Kosinov, N.A.; Pidko, E.A.; Hensen, E.J.M. Hydrogenation of Levulinic Acid to γ-Valerolactone over Fe-Re/TiO2 Catalysts. *Applied Catalysis B: Environmental* **2020**, *278*, 119314, doi:10.1016/j.apcatb.2020.119314.
152. Carroll, Z.L.; Haché, M.J.R.; Wang, B.; Chen, L.; Wu, S.; Erb, U.; Thorpe, S.; Zou, Y. Electrodeposited NiFeCoMoW High-Entropy Alloys with Nanoscale Amorphous Structure as Effective Hydrogen Evolution Electrocatalysts. *ACS Appl. Energy Mater.* **2024**, *7*, 8412–8422, doi:10.1021/acsaem.4c01316.
153. Wu, K.; Liu, C.; Li, Q.; Huo, J.; Li, M.; Chang, C.; Sun, Y. Magnetocaloric Effect of Fe25Co25Ni25Mo5P10B10 High-Entropy Bulk Metallic Glass. *Journal of Magnetism and Magnetic Materials* **2019**, *489*, 165404, doi:10.1016/j.jmmm.2019.165404.
154. Lee, C.; Song, G.; Gao, M.C.; Feng, R.; Chen, P.; Brechtl, J.; Chen, Y.; An, K.; Guo, W.; Poplawsky, J.D.; et al. Lattice Distortion in a Strong and Ductile Refractory High-Entropy Alloy. *Acta Materialia* **2018**, *160*, 158–172, doi:10.1016/j.actamat.2018.08.053.
155. George, E.P.; Raabe, D.; Ritchie, R.O. High-Entropy Alloys. *Nat Rev Mater* **2019**, *4*, 515–534, doi:10.1038/s41578-019-0121-4.

156. Bian, H.; Wang, R.; Zhang, K.; Zheng, H.; Wen, M.; Li, Z.; Li, Z.; Wang, G.; Xie, G.; Liu, X.; et al. Facile Electrodeposition Synthesis and Super Performance of Nano-Porous Ni-Fe-Cu-Co-W High Entropy Alloy Electrocatalyst. *Surface and Coatings Technology* **2023**, *459*, 129407, doi:10.1016/j.surfcoat.2023.129407.
157. Dehestani, M.; Sharafi, S.; Khayati, G.R. The Effect of Pulse Current Density on the Microstructure, Magnetic, Mechanical, and Corrosion Properties of High-Entropy Alloy Coating Fe–Co–Ni–Mo–W, Achieved through Electro Co-Deposition. *Intermetallics* **2022**, *147*, 107610, doi:10.1016/j.intermet.2022.107610.
158. Temiz, M.; Kara, A.Y.G.; Erdemir, D.; Dincer, I. More Efficient Way of Clean Hydrogen Production: The Synergetic Roles of Magnetic Effects and Effective Catalysts. *Fuel* **2024**, *376*, 132708, doi:10.1016/j.fuel.2024.132708.
159. Xiong, Z.; Ning, X.; Zhou, F.; Yang, B.; Tu, Y.; Jin, J.; Lu, W.; Liu, Z. Environment-Friendly Magnetic Fe–Ce–W Catalyst for the Selective Catalytic Reduction of NO_x with NH_3: Influence of Citric Acid Content on Its Activity-Structure Relationship. *RSC Adv.* **2018**, *8*, 21915–21925, doi:10.1039/C8RA03131B.
160. Xiao, S.; Ma, L.; An, W.; Shen, P. Stability Optimization of Iron-Based Catalysts: Application of Cr-Enriched Alloy Steel Catalyst in Ozonation Pharmaceutical Wastewater. *Separation and Purification Technology* **2025**, *354*, 129007, doi:10.1016/j.seppur.2024.129007.
161. Humphreys, J.; Lan, R.; Tao, S. Development and Recent Progress on Ammonia Synthesis Catalysts for Haber–Bosch Process. *Adv Energy and Sustain Res* **2021**, *2*, 2000043, doi:10.1002/aesr.202000043.
162. Liu, H. Ammonia Synthesis Catalyst 100 Years: Practice, Enlightenment and Challenge. *Chinese Journal of Catalysis* **2014**, *35*, 1619–1640, doi:10.1016/S1872-2067(14)60118-2.
163. Fan, H.; Ma, Y.; Chen, W.; Tang, Y.; Li, L.; Wang, J. Facile One-Step Electrodeposition of Two-Dimensional Nickel-Iron Bimetallic Sulfides for Efficient Electrocatalytic Oxygen Evolution. *Journal of Alloys and Compounds* **2022**, *894*, 162533, doi:10.1016/j.jallcom.2021.162533.
164. Kırlıoğlu, A.C.; Ölmez, B.; Rahbarshendi, F.; Buldu-Akturk, M.; Yürüm, A.; Alkan Gürsel, S.; Yarar Kaplan, B. Scalable Nano-Sized Fe-N-C Catalysts for Fuel Cells: Evaluating the Impact of Iron Precursors and CeO2 Addition. *Materials Research Bulletin* **2024**, *179*, 112952, doi:10.1016/j.materresbull.2024.112952.
165. Zhao, L.; Wang, Y.; Jin, S.; An, N.; Yan, M.; Zhang, X.; Hong, Z.; Yang, S. Rational Electrochemical Design of Hierarchical Microarchitectures for SERS Sensing Applications. *Nat. Synth* **2024**, *3*, 867–877, doi:10.1038/s44160-024-00553-1.
166. Jamal, A.; Haq, G.-U.; Hussain, S.; Gul, M.; Saifullah, M.; Anjum, M.A.R. Enhanced Tribological Properties of Electrodeposited Fe–W Alloy Coatings through Carburization. *Langmuir* **2023**, *39*, 16328–16335, doi:10.1021/acs.langmuir.3c01909.
167. Li, H.; Zhang, C.; Xiang, W.; Amin, M.A.; Na, J.; Wang, S.; Yu, J.; Yamauchi, Y. Efficient Electrocatalysis for Oxygen Evolution: W-Doped NiFe Nanosheets with Oxygen Vacancies Constructed by Facile Electrodeposition and Corrosion. *Chemical Engineering Journal* **2023**, *452*, 139104, doi:10.1016/j.cej.2022.139104.
168. Rajendiran, R.; Chinnadurai, D.; Chen, K.; Selvaraj, A.R.; Prabakar, K.; Li, O.L. Electrodeposited Trimetallic NiFeW Hydroxide Electrocatalysts for Efficient Water Oxidation. *ChemSusChem* **2021**, *14*, 1324–1335, doi:10.1002/cssc.202002544.
169. Capelli, S.; Cattaneo, S.; Stucchi, M.; Villa, A.; Prati, L. Iron as Modifier of Pd and Pt-Based Catalysts for Sustainable and Green Processes. *Inorganica Chimica Acta* **2022**, *535*, 120856, doi:10.1016/j.ica.2022.120856.
170. Hosseini, J.; Abdolmaleki, M.; Pouretedal, H.R.; Keshavarz, M.H. Electrocatalytic Activity of Porous Nanostructured Fe/Pt-Fe Electrode for Methanol Electrooxidation in Alkaline Media. *Chinese Journal of Catalysis* **2015**, *36*, 1029–1034, doi:10.1016/S1872-2067(15)60841-5.